SYNTHESIS AND CHARACTERIZATION OF DENDRITIC STRUCTURES FOR BIOMEDICAL APPLICATIONS

Adérito José Rodrigues Amaral

A thesis submitted to the Faculty of Sciences and Technology of the University of Coimbra in partial fulfillment of the requirements for the degree of Master in Biomedical Engineering

Advisers:
Prof. Doutor Jorge Fernando Jordão Coelho
Prof. Doutor Arménio Coimbra Serra

Host Institution:
Department of Chemical Engineering, Faculty of Sciences and Technology of the University of Coimbra

Coimbra
2012

Abstract

The aim of this project was the development of an alkyne-functionalized fourth generation polyester dendron, based on 2,2-bis(hydroxymethyl)propionic acid (bis-MPA), according to a double-stage convergent growth approach. The different architectures were characterized by nuclear magnetic resonance (NMR) spectroscopy and matrix-assisted laser desorption ionization time-of-flight mass spectrometry (MALDI-TOF-MS).

The [G-4] dendron attained, with a carboxylic group in its core, was subjected to several alkyne functionalization reactions that were not effective.

In this sense, a novel route to construct the polyester dendron was carried out, *via* carboxylic anhydride, and an alkyne-functionalized [G-2] dendron was successfully synthesized. To construct a [G-4] dendron, esterification and acylation reactions were performed, but the results suggested that alkyne terminal was affected.

Simultaneoulsy, alkyne functionalization reactions of poly(ethylene glycol) (PEG) were also carried out, and after several attempts, the objective was accomplished.

Although the initial purpose have not been fully achieved, the methodologies discussed and the results obtained in this study allow us to understand the chemistry behind the synthesis of dendrons. This knowledge is of utmost importance to define the future directions of the projects in this area.

Keywords: anhydride, bis-MPA, dendron, PEG

Resumo

Este projecto teve como principal objectivo o desenvolvimento de uma estrutura dendrítica de quarta geração, de base poliéster, funcionalizada com um grupo alcino.

O *dendron* de quarta geração (baseada no composto bis-MPA) foi sintetizado segundo o método *double-stage convergent growth*, tendo os resultados obtidos sido confirmados por ressonância magnética nuclear e espectrometria de massa. A estrutura sintetizada, com um grupo carboxílico no seu 'núcleo', foi sujeita a diversas reacções de funcionalização com terminais alcino, revelando-se, no entanto, infrutíferas.

Deste modo, um novo método, através do anidrido carboxílico, foi testado e um *dendron* de segunda geração, funcionalizado com o grupo alcino, foi sintetizado com sucesso. Com o mesmo intuito de construir uma estrutura de quarta geração, reacções de esterificação e acilação foram executadas, mas os resultados obtidos sugerem que o terminal alcino, presente inicialmente, foi afectado.

Concomitantemente, reacções de funcionalização do polietilenoglicol com um terminal alcino foram também realizadas, tendo sido sintetizado com sucesso (após várias tentativas).

Embora o objectivo inicial não tenho sido totalmente alcançado, as metodologias abordadas e os resultados obtidos neste projecto, permitem retirar algumas ilações acerca do processo de síntese de estruturas dendríticas. Este conhecimento reveste-se de especial importância na definição de novas estratégias que devem ser adoptadas futuramente.

Palavras-chave: anidrido, bis-MPA, PEG

Acknowledgements

I would like to express my appreciation to my advisers, Prof. Doutor Jorge Coelho, Prof. Doutor Arménio Serra and Mestre Joana Góis, for all the knowledge transmitted. Their guidance and helpful discussions were essential. I am also grateful to the collaborators I have worked with, for all the support and for providing stimuli-responsive polymers.

Aos meus Pais, banco privado de crédito, e à Avó Prazeres, responsável máxima dos departamentos de restauração e limpeza.

Coimbra, 2012

Contents

List of Figures

List of Tables

List of Abbreviations

AA Acrylic acid

bis-MPA 2,2-Bis(hydroxymethyl)propionic acid

CDI 1,1'-Carbonyldiimidazole

CMC Critical micelle concentration

CMT Critical micelle temperature

CuAAC Copper-catalyzed azide/alkyne cycloaddition

DCC *N,N'*-Dicyclohexylcarbodiimide

DDS Drug delivery systems

DIC *N,N'*-Diisopropylcarbodiimide

DMAP 4-(Dimethylamino)pyridine

DMF *N,N*-Dimethylformamide

DPTS 4-(Dimethylamino)pyridinium p-toluenesulfonate

EBiB Ethyl 2-bromoisobutyrate

EDC *N*-(3-Dimethylaminopropyl)-*N'*-ethylcarbodiimide hydrochloride

EPR Enhanced permeability and retention

EtOAc Ethyl acetate

FRP Free radical polymerization

FT-IR Fourier transform - infrared spectroscopy

HABA 2-(4-hydroxyphenylazo)benzoic acid

HCCA α-cyano-4-hydroxycinnamic acid

LCST Lower-critical solution temperature

LDBC Linear-dendritic block copolymer

LRP Living radical polymerization

MAA Methacrylic acid

MALDI-TOF-MS Matrix-assisted laser desorption ionization time-of-flight mass spectrometry

m/z Mass-to-charge ratio

NMR Nuclear magnetic resonance

PAMAM Poly(amidoamine)

Pd/C Palladium on carbon

PDI Polydispersity index

PDIPAEMA Poly(2-(diisopropylamino)ethyl methacrylate)

PDMAEMA Poly(2-(dimethylamino)ethyl methacrylate)

PEI Poly(ethylene imine)

PEG Poly(ethylene glycol) methyl ether

PMDETA *N,N,N',N",N"*-pentamethyldiethylenetriamine

PNIPAAm Poly(N-isopropylacrylamide)

PPI Poly(propylene imine)

PVCa Poly(N-vinyl caprolactam)

RES Reticuloendothelial system

RT Room temperature

T_g Glass transition temperature

THF Tetrahydrofuran

TLC Thin-layer chromatography

TMS Tetramethyilsilane

TsOH p-Toluenesulfonic acid

1

Introduction

Cancer is one of the most challenging medical problems faced by science today. According to the *International Agency for Research on Cancer*, in 2008, around 12.7 million new cases were registered and the total cost of treatment amounted to over 890 billion dollars[7].
Therefore, improving our knowledge of cancer pathophysiology, discovering new anticancer drugs and developing novel biomedical technologies are of utmost importance nowadays.

New developments in targeted drug delivery methods can be a promising alternative: dendrimers are a class of nanoparticles that are being explored in this sense.

The aim of this project included initially five main tasks:

1. Task I

    . The synthesis of an alkyne-functionalized [G-4] aliphatic polyester dendron based on bis-MPA, using a double-stage convergent growth approach;

2. Task II

    . The covalent attachment of a stimuli-responsive linear polymer prepared by 'controlled'/living radical polymerization, using a 'click' chemistry approach;

3. Task III

    . The assess of the self-assembly behaviour of the amphiphilic linear-dendritic block copolymer prepared, under different pH and temperature conditions;

4. Task IV

    . Alkyne functionalization of poly(ethylene glycol) methyl ether (Mn $\sim$ 2000) and synthesis of linear-linear block copolymer through 'click' chemistry;

5. Task V

    . Self-assembly studies of the amphiphilic linear-linear block copolymers.

Unfortunately, the initial plan was too ambitious due to the several difficulties encountered during the accomplishment of the first task. For this reason, tasks II, III and V weren't performed.

Therefore, in the present work, we intend to describe and discuss the several synthesis methodologies carried out - double-stage convergent growth and anhydride route - to attain the fourth generation polyester monodendron with the final core functionalized by an alkyne moiety.

At the same time, poly(ethylene glycol) methyl ether alkyne functionalization reactions are also discussed as well as 'click' reactions attempts.

The general proceedings of the present work are chronologically represented in the timetable from Figure 1.1.

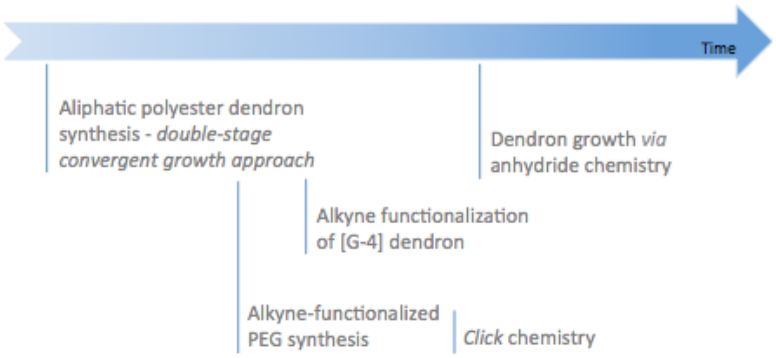

Figure 1.1: Condensed timetable of project proceedings.

In the second chapter of this dissertation, it will be highlighted the main properties of drug delivery systems and how they can be applied in medical and pharmaceutical fields. Furthermore, it will be made a brief review about the state of art of dendritic polymers and stimuli-responsive polymers. Structural characteristics of linear-dendritic block copolymers, their synthesis methodologies and some biocompatibility aspects will be also discussed.

In the third chapter, the different synthesis methodologies performed will be described. The materials as well as the characterization techniques used in order to characterize the synthetic structures will be presented.

In the fourth and fifth chapters, the experimental results will be compared and discussed. Finally, overall conclusions and guidelines for future work in this field will be suggested.

2

Theoretical Background

2.1 Drug delivery systems

Often, we imagine that our body can be mended and improved through the addition of chemicals, but we don't really understand the identity of all of them in the system, the forces that hold them together or the network of interactions that mold the chemicals into the organism. This is the challenge of drug delivery.

There are several forms of drug administration such as pills, injections, suppositories, and all of them have been already experimented by most people.

These conventional drug delivery methods result in a peak in plasma drug concentrations, followed by a plateau and finally a decline. As a result, these common formulations require a high concentration of the drug at the time of the release, but only a small dose reaches the desired location. Therefore, it is necessary the administration of higher dosages than required to achieve the desired therapeutic effect, which may lead to toxic plasma drug concentrations or ineffective plasma levels[8]. Although these systems maintain the drug within the desired therapeutic range with just a single dose, they remain insensitive to the changing metabolic states of the body.

In this sense, mechanisms capable of responding to these physiological variations must be provided in order to synchronize drug-release profiles with changing physiological conditions.

Controlled drug delivery systems (DDS) allow gradual and prolonged release of the active compound in a specific tissue, maximizing the therapeutic index and reducing the adverse effects. Ideally, they should respond to physiological requirements, sense the changes and alter the drug-release profile accordingly[9].

Their biggest advantages are depicted in Figure 2.1: reduction of dosing frequency, controlled release rate of drug during a pre-defined time period and maximization of therapeutic index to avoid an overdose or underdose[1].

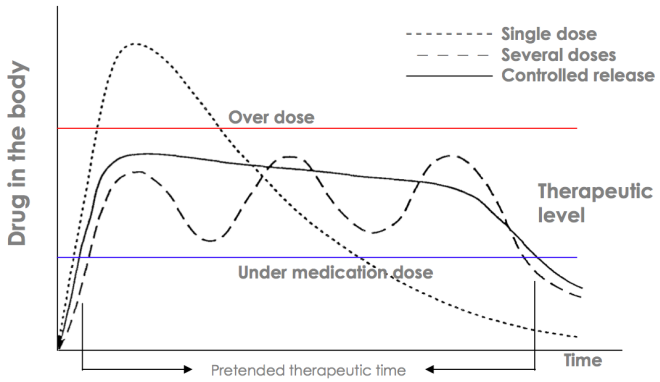

Figure 2.1: Patterns of drug concentration after administration by conventional methods (e.g., single dose and several doses) and by controlled drug delivery systems (adapted from[1]).

The different pathophysiological conditions of diseases continually call for innovative therapeutic approaches. The development of polymeric DDS is always dependent on a thorough knowledge of physical, chemical, morphological and biological properties of the polymer and therapeutic agent.

The versatility of polymeric materials allow us to design innovative systems with distinct characteristics at structural and functional levels, through the tailor of molecular weight, addition of bioresponsive elements, control of the size, shape, composition, chemical functionality and self-assembly process[10].

Throughout the development process, it is necessary to address all the biological safety requirements of a drug-polymer carrier: they should be water soluble, biocompatible, biodegradable and bioactive[11]. Besides, DDS should also address the following criteria: high drug loading capacity, adequate binding affinity and stability in the blood stream, long time circulation properties, suitable release kinetics along with selective bioactive agent distribution pattern[10].

Fast degradation, unfavorable distribution, elimination by glomerular filtration and side effects are problems that drug administration face. So, when designing drug delivery carriers for biomedical applications, there are numerous aspects to be consider such as prolong circulation half-time of the drug, promote target delivery, maximize drug bioavailability, minimize side effects and improve therapeutic efficacy.

Control key aspects of biodistribution and cellular internalization is extremely important. The development of molecular nanostructures with well defined shape and size is of eminent interest in medical field for the delivery of active pharmaceuticals agents[11].

2.2 Therapeutic applications

Cancer

In the past years, therapeutic agents used in conventional chemotherapy are plagued by lack of selectivity associated with low therapeutic index. In this sense, tumour-targeting DDS offer themselves as an alternative.

The primary goal of these approaches relies on the accumulation of engineered nanoparticles in solid tumour tissue due to the enhanced permeability and retention (EPR) effect[12].

In contrast with healthy tissue, the fast development of vasculature in tumour tissue, by abnormal angiogenesis, lead to an hyperpermeability of the endothelial cells owing to the inherent pores in the vessel walls (with an average size of ~ 400 nm). These intercellular gaps in tumour vasculature allow nanoparticles to escape from the circulation and to extravasate into the tumour (passive targeting). Moreover, the lack of lymphatic drainage lead to the accumulation of macromolecular drugs in the interstitium of tumours[13].

To capitalize on the EPR effect, a high concentration of the drug in the systemic circulation as a function of time should be achieved to maximize diffusion out of the leaky blood vessels into tumour tissue. The encapsulation of an active agent confer enhanced solubility, cellular uptake, intestinal absorption and physical stability. Thus, a prolonged circulation and improved tumour accumulation of the drug is attained, enhancing anti-tumour efficacy (compared with the free drug) and increasing the therapeutic window[13]. Besides, the polymer molecular weight of the polymer-drug conjugate can be tuned to take advantage of this effect.

One of the crucial points in this process is the efficiency of the carrier to release the drug in the target tissue, ideally, few minutes after their internalization through the mechanism of endocytosis. The acidic media of the endossome act as a trigger: dissociate the nanocarrier and release the drug.

The size of the nanoparticles is an important factor in controlling the biodistribution of the drug in the human body; it influences particle uptake, deposition and clearance. Drug carriers should have a diameter larger than 3 nm to prevent rapid clearance by the kidneys but smaller than 200 nm to avoid the reticuloendothelial system (RES) (ideally $\sim 10 - 100$ nm)[14].

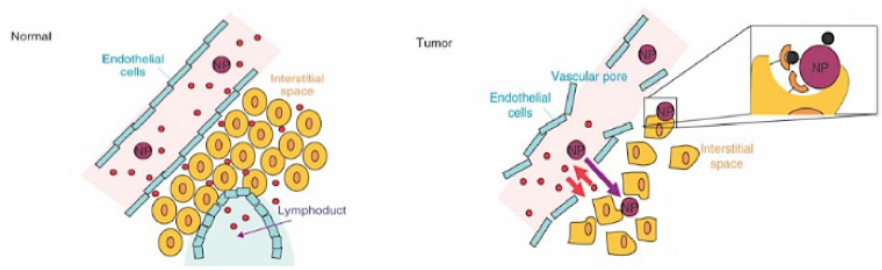

Figure 2.2: Schematic of the EPR effect (adapted from[2]). Tumour vessels are structurally irregular and leaky compared to normal vessels. Endothelial cells can't form a normal monolayer, overlap and nanoparticles enter through the gaps in the tumour vasculature.

It should be also noted that vessel permeability varies during tumour progression (due to a high interstitial fluid pressure) which can decrease the ability of particles to extravasate[15].

The surface properties of the drug carrier are also crucial in determining the biocompatibility, biodistribution and retention within the circulatory system.

The modification of the nanoparticle surface with hydrophilic moieties, like PEG, creates a hydrodynamic barrier that prevents recognition and uptake by the RES, reducing the toxicity of the carrier and increasing its circulation half-life[16].

Cancer cells often display increased cell surface expression of proteins that may be found at low levels on normal cells as well as proteins that are found exclusively on cancer cell surfaces. In this sense, chemical attachment of a cell-specific ligand to the surface of the carrier that strongly interacts with antigens (or receptors) displayed on the target tissue, can introduce a specific (active) targeting to the drug-encapsulating nanoparticle[15].
The use of a targeting moiety decreases adverse side effects by allowing the drug to be delivered to the specific site of action and facilitates cellular uptake of the drug by receptor-mediated endocytosis. Folate, transferrin and Luteinizing hormone-releasing hormone are examples of targeting ligands reported in literature[17].

2.3 Dendritic polymers

2.3.1 Fundamentals

Dendritic polymers constitute a recent and attractive family of polymers with unique structures and properties. Based on their branched controlled structure, dendritic polymers can be classified into four main subgroups: hyperbranched polymers, dendrigrafts, dendrons and dendrimers[3]. These dendritic architectures are closely related to each others but reflect the level of control over the branching units used to synthesize these assemblies.

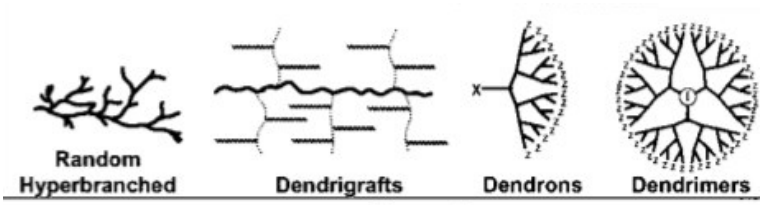

Figure 2.3: Representation of dendritic architectures (adapted from[3]).

The first dendritic wedge was reported by Vögtle et al.[18], in 1978, describing the synthesis of 'cascade molecules'. In 1985, Tomalia group proposed the term 'dendrimer' to describe a unique core-shell macromolecular architecture[19]. The term 'dendrimer', originates from the Greek, is a combination of the words *dendron* = tree and *meros* = part, and it was chosen due to its treelike structure that may be found in innumerable examples in nature[20].

Dendrimers (or arborols) are multivalent macromolecules characterized by a regular, globular and highly branched structure. One of the most attractive properties of this architecture is the large number of peripheral groups that may be modified to afford polymers with tailored properties.

Their distinct topology offers unique properties when compared to traditional linear polymers. Generally, they are more soluble in common solvents compared to analogous linear polymers (increased free volume and peripheral groups)[21]. Solubility characteristics of dendrimers depend mainly on the nature of the peripheral groups. Dendrimers terminated in hydrophilic groups are soluble in polar solvents, while dendrimers having hydrophobic end groups are soluble in nonpolar solvents.
Physical properties like viscosity and thermal behaviour also differ significantly. The viscosity in solution is significantly lower than linear analogues. For instance, studies conducted show that intrinsic viscosity decreases with

higher generation dendrimers[22]; this behaviour is assigned to the transition from an extended structure to a compact globular shape. The increase in the number of end-groups lowers the glass transition temperature (T_g), that comes closer to a final value after higher generations. Hawker and Chu demonstrated that thermal properties also strongly depend on the properties of the terminal groups[23].

Dendrimers have a three-dimensional well defined multi-branched architecture with low polydispersity index (PDI) due to the high degree of control over the process of synthesis that provides monodisperse polymers (dendigraft and hyperbranched polymers are less controlled)[24]. Due to their globular shape and the presence of internal cavities, dendrimers offer the possibility to encapsulate guest molecules in the macromolecule interior[25]. Therefore, a tremendous progress in the chemistry of dendrimers has been observed, shifting the interest to the potential applications of these polymeric materials: catalysis, sensors, micelles and encapsulation, contrast agents, liquid crystalline materials, among others[21].
The structural diversity in the repeat units is impressive and a wide variety of architectures have been created, including poly(amidoamine) (PAMAM), poly(propylene imine) (PPI), polyether and bis-MPA based dendrimers[26].

Dendrimers structure consists of three basic architectural components: the core, the interior and the end-groups (see Figure 2.4).

The core is positioned at the center and to it branched wedges are attached. The number of branched points encountered upon moving outward from the core to the periphery represents the generation number. Increasing the number of generations, higher branching density and wider structures will be created with amplification of the peripheral functionalities.

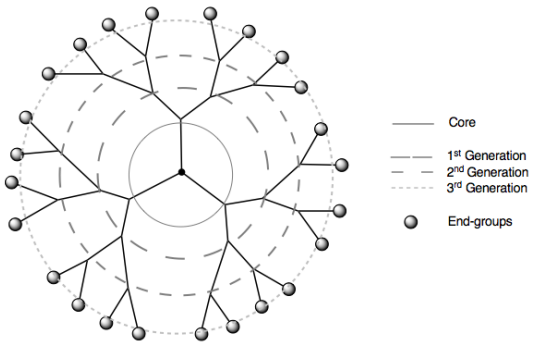

Figure 2.4: Schematic representation of a dendrimer.

Dendrimers can be tailored by the nature of the core, the type of building blocks and the functional groups at the periphery. Physical and chemical

properties as well as overall size, shape and flexibility are strongly influenced by each one of this architectural component that exhibits a specific function at the same time that defines unique properties for these nanostructures, as they grow generation by generation[24].

The surface groups with appropriate functionalization allow the modulation of interfacial properties and the interaction with the surrounding environment, enhancing the biocompatibility and enabling the design of multifunctional dendrimers[27]. They may also act as reactive gates controlling the releasing of guest molecules from the interior of the dendrimer.

The higher degree of control over the highly branched structure and the ability to tailor dendrimers properties to therapeutic needs (reducing experimental and therapeutic repeatability) make them ideal for targeted drug-delivery, macromolecular carriers, surface engineering and biomimetic applications[28].

2.3.2 Synthesis methodologies

Dendrimers synthesis requires multi-step synthetic routes with laborious and time consuming activation/protection steps, condensation reactions and purifications processes to remove excess of reagents and byproducts, since is the only way to achieve overall control over the final structure[21].

For the synthesis of dendrons and dendrimers by step-by-step sequences, two main strategies have emerged: the convergent and the divergent growth approaches (see Figure 2.5). In both ways, dendrimers can be prepared with high precision and controlled molecular weight[4]. Based on the characteristics of the target molecule, the chemical steps during the synthesis and the building blocks used in the design of the dendritic structure, the choice of a synthetic route is done[29].

Both methods require two steps for the growth of each generation: the activation of the dendritic unit and the addition of new monomer.

In the divergent approach, pioneered by Newkome[30] and Tomalia[19] in 1985, the dendrimer grows radially outwards from a multifunctional core site by repetitive cycles of addition of molecules, layer-by-layer.
The increase number of terminal groups of every layer aggravate the addition of new monomer at higher generations due to a sterically hindered surface. Problems may occur from side reactions and incomplete reactions that lead to structural defects, causing difficulties when purifying these materials. Thus, excess of reagent and full substitution of the end-groups through deprotection/activation reactions are needed to afford regular branching[29]. The first PAMAM dendrimers were synthesized by this approach[24].

In the convergent approach, developed by Hawker and Fréchet[31], dendrimer is constructed stepwise, starting from the periphery inward to a focal point. Dendrons are synthesized separately and in a final step coupled to a

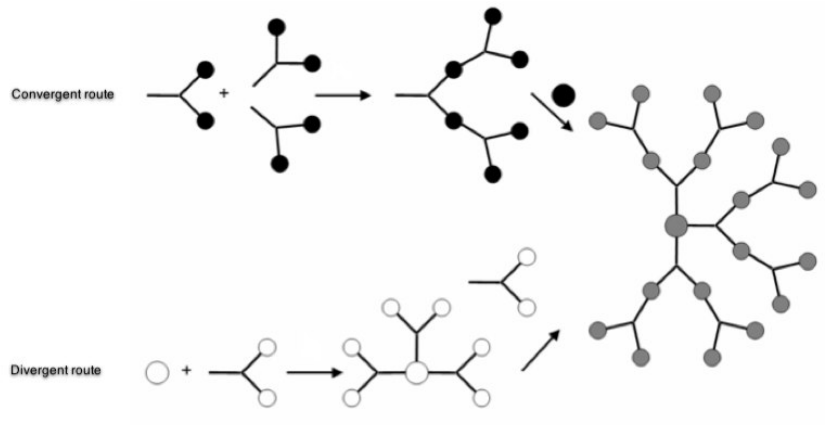

Figure 2.5: Schematic representation of convergent and divergent synthetic routes.

multifunctional core molecule to afford the final dendrimer.

The advantages of this strategy are the precise control in each step of the dendritic structure and the simpler purification procedures due to the difference in molecular weight and polarity between products and byproducts[32]. However, this method is usually limited to dendrimers of lower generations due to steric hindrance that potentially difficult the last coupling step in large dendrons[28].

Considering the large number of steps involved in the synthesis and purification of higher generation dendrimers as well as their time-consuming synthesis, it is desirable to reduce the number of synthetic steps and to improve the overall yield of the final dendrimer.

This could be achieved in a double-stage convergent growth approach, where the monodendrons containing a single reactive group at the focal point are coupled in a divergent manner to the periphery of a dendron prepared by a convergent or divergent growth approach[4] (see Figure 2.6).
This approach enhance the versatility of the synthesis, reduce the number of growth steps and facilitate the purification of the final product.

2.3.3 Biocompatibility

A major concern when introducing a new class of nanoparticles for medical applications is directed towards the biocompatibility of these particles. In order to use them in drug delivery applications, dendrimers have to fulfill certain requirements: non-toxic, non-immunogenic and biodegradable.

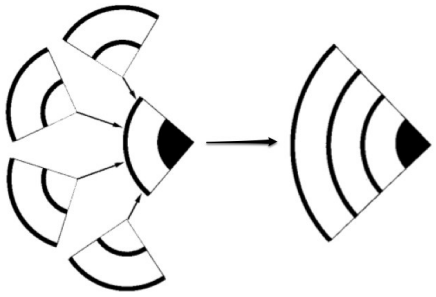

Figure 2.6: Schematic representation of a double-stage convergent growth approach of a dendron (adapted from[4]).

Moreover, they should be able to circulate in the body for the time needed to have a clinical effect and display an inherent body distribution that will allow appropriate tissue targeting[33].

The nature of the dendrimers end-groups dictate whether or not it displays a significant toxicity. A difference was observed between the toxicity of cationic dendrimers and neutral or anionic dendrimers. Studies shown that PAMAM and PPI dendrimers with terminal primary amines generally display concentration-dependent toxicity and haemolysis whereas dendrimers containing neutral or anionic groups had shown to be less toxic and haemolytic; lower-generation PAMAM dendrimers with carboxylate end-groups show neither haematotoxicity nor cytotoxicity at concentrations up to 2 mg/ml[34]. It was also clarified that biocompatibility of dendrimers is not only determined by the surface groups: dendrimers containing an aromatic core may cause haemolysis through hydrophobic membrane contact.

In this sense, it is of interest to develop and assess novel water-soluble and biocompatible dendritic structures. Studies of polyester-based dendrimers based on bis-MPA were carried out and showed a low toxicity profile both *in vitro* and *in vivo*. Since the dendrimer may be degraded by hydrolytic enzymes after the release of the drug, this system is a promising polymeric backbone in the development of well-defined drug carriers[35].

2.4 Stimuli-responsive polymers

Stimuli-responsive polymers (or smart polymers) are materials that reversibly change their physicochemical characteristics in response to a narrow variation in surrounding environmental conditions. Stimuli, such as pH, temperature, ionic strength, electromagnetic radiation, mechanical forces,

magnetic and electric fields can lead to different type of responses: degradation, swelling/collapsing, conformational change, drug release, among others[36].

Progressive developments in polymerization techniques allow the design of smart polymers with controlled molecular weight, architecture and properties that define the polymer response[1].

Nanocarriers systems with triggering mechanisms offer great advantages in drug delivery for biomedical applications. While traditional systems act exclusively as passive drug carriers, these systems undergo changes in their nature in response to pathological triggers that stimuli the drug release. This feature lead to a maximal therapeutic efficacy at the disease site while reduce undesired side effects[5].

Although several smart polymers have been exploited, most of the work reported is related to pH- and temperature-responsive polymers, mainly, because these properties are important physiological indicators and are easily controlled.

This strategy allow us to aim further for tailor-made DDS with superior pharmacokinetics while having all safety questions addressed (e.g., problems associated with traditional chemotherapy).

2.4.1 Temperature-responsive polymers

Since temperature is one of the most important physiological indicators, any deviation from normal values can act as a trigger for temperature-responsive polymers.

These polymers exhibit a volume phase transition at a critical solution temperature which causes a change in the solvation state (leading to the formation of hydrophobic domains)[36]. The polymer chain collapse or extend, responding to hydrophobic and hydrophilic interactions between the polymer and the aqueous medium[1].

Typically, thermo-responsive polymers are soluble, in aqueous solution, below their lower-critical solution temperature (LCST) due to the hydrogen bounding with water molecules (expanded state). Upon heating, they become insoluble and dehydrated (compact globule)[37]. Above the LCST, intra- and intermolecular interactions between the hydrophobic molecules are favored compared to a solubilisation by water molecules and the polymer undergoes an abrupt change in the specific volume[38] (see Figure 2.7). The balance between the hydrophilic and hydrophobic groups along the polymer chain determines the LCST.

Thermal responsive character of these polymers broadens the possibilities of DDS applications. For example, body-site temperature can change

upon local infection and therapeutic agents may be release as result of a trigger if the LCST of the material is close to body temperature.

Mild clinical hyperthermia (42 °C) damage cancer cells or make them more sensitive to the effects of radiation and anticancer drugs. It also affects the biological functions of cancer cells (e.g., decreased DNA synthesis, disrupted microtubules, altered receptor expression) without biological damage to normal cells[39].
So, the combination of thermo-responsive polymers with local hyperthermia condition at the solid tumour could provide more effective treatment.

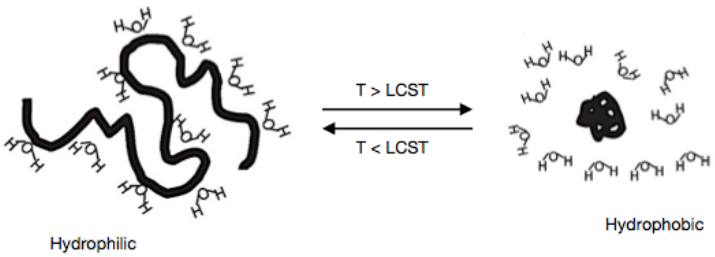

Figure 2.7: Polymer response to temperature (adapted from[5]).

Poly(N-vinyl caprolactam) (PVCa) and poly(N-isopropylacrylamide) (PNIPAAm) are examples of temperature sensitive polymers reported.

PVCa possess very interesting properties for biomedical applications: biocompatibility, low toxicity, high absorption ability, solubility in water and organic solvents (due to the presence of hydrophilic and hydrophobic groups in its structure) and LCST close to the body temperature (32 °C)[40;41].

PNIPAAm has been used, for example, in drug targeting, thermo-sensitive coatings or micelles for controlled release of drugs[42]. It exhibits a LCST around 32 °C (pH $\sim$ 7) and it is, probably, the most used macromolecule in temperature-responsive hydrogels. Above this temperature, a reversible conformational transition occurs from expanded coil (soluble) to compact globule (insoluble). Its distinctive behaviour is attributed to the rapid alteration of hydrophilicity. The amphiphilic chains hide the hydrophilic amide groups and expose the hydrophobic isopropyl groups in the compact globule conformation[43].

Despite promising studies, PNIPAAm is not the ideal candidate for biomedical applications due to its non-degradable, insoluble nature and unclear effect in the body[44].

2.4.2 pH-responsive polymers

pH variations within the body can be also used as a tool for drug carriers systems. pH-responsive polymers have been proposed for different biomedical applications, especially for entrapment and delivery of bioactive agents (since different organs or tissues have specific pH)[43].

These polymers have weak acid or basic functional groups (e.g., carboxylic acids, amines, etc.) attached to the backbone. The ionization state of the pendant group changes upon variation of the pH causing a modification of the water solubility of the chains[1].

The aqueous solubility of a pH-responsive polymer depends on the pH of the solution because variation around the pK_a value causes protonation or deprotonation of the polymer chains[45].

For example, carboxylic pendant groups of poly(acrylic acid) at low pH accept protons, while release them above its pK_a (4.28). Therefore, the polymer exhibits a collapsed conformation at low pH and an expanded state at high pH. The opposite effect is observed for polybases[43].

To attain pH sensitive polymers, the most explored monomers are acrylic acid (AA) and methacrylic acid (MAA). Poly(ethylene imine) (PEI) and poly(2-(diisopropylamino)ethyl methacrylate) (PDIPAEMA) are also examples reported in literature[36].

Poly(2-(dimethylamino)ethyl methacrylate) (PDMAEMA) is an example of a dual temperature/pH-responsive polybase (respond independently and simultaneously to temperature, $38 - 40\,^{\circ}\mathrm{C}$, and pH, pKa ~ 2.5).

Tumour tissue (as well as inflamed or wound tissue) exhibits a extracellular pH more acidic ($\sim 6.5 - 7.2$) when compared to the normal physiological extracellular pH ($\sim 7.35 - 7.45$)[36]. In this sense, responsive systems can be useful to release bioactive agents by pH-triggering at the physiological environment.

For instance, in non-viral gene therapy, the intracellular delivery of nucleic acids usually uses cationic polymers which complex the negatively charged molecules. Once the target tissue is reached, cellular uptake of the complex take place through pinocytosis or receptor-mediated endocytosis. In response to the acidification of the medium, the polycations trigger endossome membrane disruption and release its content into the cytosol due to the proton-sponge effect (see Figure **??**)[36].

2.5 Linear-dendritic block copolymers

2.5.1 Structural characteristics

Bioinspired smart block copolymers represent a new class of functional materials with tremendous applications in drug delivery.

Amphiphilic block copolymers consist of at least of an hydrophobic segment attached to an hydrophilic segment. In solution, the amphiphilic block copolymer chains tend to organize themselves into various ordered structures when the critical micelle concentration (CMC) and/or the critical micelle temperature (CMT) are achieved. Spherical micelles are the most common self-assemble structures, among the many supramolecular structures possible, and are promising drug delivery carriers for hydrophobic therapeutic agents.

From the combination of dendritic structures with linear segments, it is possible to design unique biomimetic hybrids with novel macromolecular architectures such as linear-dendritic block copolymers (LDBC), rod coils or multi-arm star polymers[46–48].
This hybrid system combines the advantages of regular spherical dendrimers with the phase segregation behaviour of traditional linear block copolymers. The macromolecular system is biocompatible and biodegradable, provides a high density functional surface that can be used to cluster ligands for efficient targeting and sensing capabilities and forms extremely stable micelles with an unusual low CMC due to the semirigid rod nature of the comb block that takes a unique cone shape, yielding self-assembly behaviour[6].

By tuning the chemical nature, size and length of the blocks, a broader extent of controlled properties can be obtained.

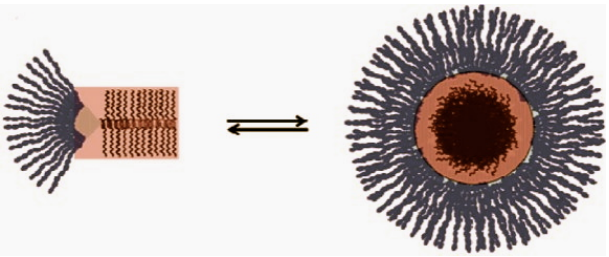

Figure 2.8: Formation of micelles from a amphiphilic linear-dendritic diblock copolymer (adapted from[6]).

2.5.2 Synthesis methodologies

Living radical polymerization

Living radical polymerization (LRP) emerged to overcome the limitations of the conventional free radical polymerization (FRP). This method combines the advantages of the FRP, such as easy procedure, water-friendly and compatibility with several functional monomers with the ability of the synthesis of well-defined polymers, due to a strict control over the macromolecular properties - molecular weight distribution, chain length, topology, composition, functionality and architecture [49;50].

Controlled LRP strategies rely on the dynamic equilibrium between growing radicals and dormant species, based on a fast activation/deactivation process. This mechanism decreases the number of growing radicals compared to the traditional FRP [51]. Therefore, the living character of the polymer chains allows further reinitiating by adding new monomers, which leads to the easy preparation of controlled block copolymers.

'Click' chemistry

This concept was first introduced by Sharpless in 2001 with the aim of binding two molecular blocks together in an easy, selective and high-yield reaction, under mild conditions with no byproducts [52]. Among the several 'click' reactions reported, the most used that can fulfill these conditions is the copper-catalyzed azide/alkyne cycloaddition (CuAAC) [53].

One specific cycloaddition reaction is the 1,3-dipolar cycloaddition between azido and alkynyl groups in the presence of copper (I) salts yielding 1,4-disubstituted 1,2,3-triazoles (see Figure 3.3). This 'click' chemistry reaction has recently proved to be a very powerful synthetic tool due to its easy procedure, high selectivity and conversion (obtained under mild reaction conditions) [54]. However, the copper component may be a problem if traces remain under physiological conditions.

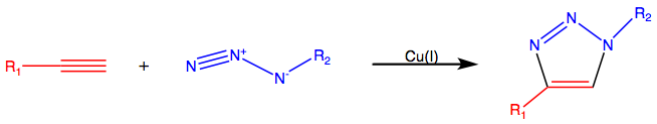

Figure 2.9: 1,3-dipolar cycloaddition between azido and alkynyl groups catalyzed by copper salts.

'Click' reactions are a useful tool not only for LDBC synthesis but also in functionalization strategies[55]. Applications are largely expanding in the fields of organic synthesis, dendritic polymers (e.g., surface functionalization of dendrimers, molecular recognition and nanoparticle catalysis) and biomacromolecules[56].

Indeed, the CuAAC reaction is a suitable solution to several problems in polymer science: reaction conditions are more attractive than conventional, purification is easier and the triazole 'bridge' is considered to be biologically stable.

3

Experimental Section

3.1 Characterization techniques

3.1.1 Nuclear magnetic resonance

Nuclear magnetic resonance (NMR) spectroscopy exploits the magnetic properties of certain atoms, studying the transitions between different quantized energy levels when an external magnetic field is applied. This technique allows qualitative and quantitative analyses of compounds mixtures and determination of molecular structures, due to the dependence of frequency and intensity of signals with the molecular architecture of the sample.

Hydrogen (^{1}H), carbon (^{13}C) and fluorine (^{19}F) nuclei are frequently used in NMR spectroscopy analysis. For instance, ^{1}H nucleus has a high relative abundance and it is very sensitive to the presence of external magnetic fields. To perform this analysis, deuterated solvents are frequently used such as chloroform-d ($CDCl_3$) or water-d_2 (D_2O)[57].

The resulting NMR spectrum present several absorption peaks, providing helpful information (number, position and intensity of signals) about the molecular structure of the compounds, that will be discussed below.

Protons with different environments absorb to different magnetic inductions. Thus, the number of signals in the spectrum translates the number of protons chemically equivalent that exist in the molecule.

The position of the signals in the NMR spectrum is a source of information about the electronic environment of each specie of protons. The reference point is generally the signal of tetramethyilsilane (TMS), whose protons are chemically equivalent causing a narrow single signal at position 0.0. The chemical shift (δ), or offset, characterizes a proton in its environment and corresponds to the position of an absorption peak in relation to the reference. So, chemically equivalent protons have the same chemical shift and the more protected are the nuclei, the smaller the chemical shift is (and vice

versa).
The signal intensity depicts how many protons of each specie exist in the molecule. The area below each peak (integration) is proportional to the number of protons that triggered the signal[58].

3.1.2 Fourier transform - infrared spectroscopy

Infrared spectroscopy is a characterization technique widely used to assess the light absorbed by a sample at each wavelength of the infrared spectrum, allowing the characterization of chemical processes (e.g., vibration of interatomic bonds) and molecular structure. When a sample is exposed to infrared light, it absorbs radiation at certain frequencies that are characteristic of the chemical bonds present in the molecule. Thus, an infrared spectrum represents the *fingerprint* of a sample with absorption peaks which correspond to the frequencies of vibrations between the bonds of the atoms that makeup the compound, leading to a qualitative analysis.

Fourier transform - infrared spectroscopy (FT-IR) has a high sensitivity, resolution and short scan time. Generally, sample analysis is performed in reflectance or transmission modes. In the second case, matrix isolation techniques (e.g., KBr or CsI) are needed to prepare the sample. In the first one, samples can be examined directly in the solid or liquid state without further preparation.
Attenuated total reflectance (ATR) operates by measuring the changes that occur in a totally internally reflected beam when it comes into contact with the sample. An infrared beam is directed onto a crystal (with a high refractive index) in such a way that it reflects off the internal surface in contact with the sample. This internal reflectance creates an evanescent wave that extends beyond the surface of the crystal into the sample[57].

3.1.3 Matrix-assisted laser desorption ionization

Matrix-assisted laser desorption ionization is an analytical mass spectrometry technique that measures the mass-to-charge ratio (m/z) of ions, allowing the analysis of biomolecules and organic macromolecules (e.g., dendrimers, hyperbranched polymers, etc.). In time-of-flight method, ions are bombed by a high-energy electron beam, ionize and cleave. The time it takes for the ions to travel from the analyzer to the detector is measured and is proportional to their m/z (linear mode). Each set of ions formed has a certain value of m/z and the intensity of each signal reflects the relative abundance of the ion that produces it.

In this sense, MALDI-TOF-MS allow the determination of the molecular weight, formula, and can assess the presence of structural units whithin the

molecule[58].

3.2 Materials

bis-MPA (98%, Aldrich), 2,2-dimethoxypropane (98%, Sigma-Aldrich), sodium sulfate (Na_2SO_4) anhydrous (JMGS, Lda), Dowex 50WX2-200 H^+-exchange resin (Sigma-Aldrich), *N,N'*-Dicyclohexylcarbodiimide (DCC) (99%, Aldrich), benzyl bromide (98%, Aldrich), pyridine ($\geq$ 99%, Sigma-Aldrich), silica 60A 60μm-200μm chromatography (Fisher Scientific), TLC silica gel 60 F_{254} (Merck Chemicals), deuterated chloroform ($CDCl_3$) (99.96%, Aldrich), palladium on carbon (Pd/C) 10 wt.% (Aldrich), propargyl bromide solution (80 wt.% in toluene, Aldrich), potassium hydroxide (KOH) ($\geq$ 85%, Sigma-Aldrich), *N,N'*-Diisopropylcarbodiimide (DIC) (99%, Aldrich), propargylamine (98%, Aldrich), propiolic acid (95%, Aldrich), *N*-(3-Dimethylaminopropyl)-*N'*-ethylcarbodiimide hydrochloride (EDC) ($\geq$ 98%, Fluka), 1,1'-carbonyldiimidazole (CDI) ($\geq$ 97%, Aldrich), 4-pentynoic acid (98%, Acros Organics), 3-butyn-1-ol (98%, GFS Chemicals), 4-pentyn-1-ol (95%, Acros Organics), sodium hydroxide (NaOH) (Merck Chemicals), sodium chloride PA (Panreac), celite hyflo super cel (Panreac), sodium hydride (60%) (NaH), 2-(4-hydroxyphenylazo)benzoic acid (HABA) (99.5%, Sigma-Aldrich), α-cyano-4-hydroxycinnamic acid (HCCA) (99.5%, Sigma-Aldrich), *N,N*-Dimethylformamide (DMF) (99%, Fisher Scientific), hexane (JMGS, Lda), ethyl acetate (EtOAc) ($\geq$ 99.97%, Fisher Scientific), 1,2-dichloroethane (Fluka), toluene (99.9%, Fisher Scientific), diethyl ether (Panreac) and methanol (JMGS, Lda) were used as received (without further purification).

Triethylamine ($\geq$ 99.0%, Sigma-Aldrich), dichloromethane (CH_2Cl_2) ($\geq$ 99.99%, Fisher Scientific), tetrahydrofuran (THF) ($\geq$ 99.97%, Fisher Scientific) and acetone (JMGS, Lda) were distilled before used. p-toluenesulfonic acid monohydrate (TsOH) ($\geq$ 98.5%, Sigma-Aldrich) and poly(ethylene glycol) methyl ether Mn $\sim$ 2000 (Aldrich) were dried by azeotropic distillation in toluene. 4-(Dimethylamino)pyridine (DMAP) (99%, Aldrich) was purified by recrystallization.

4-(Dimethylamino)pyridinium p-toluenesulfonate (DPTS) was synthesized according to the general procedure developed by Moore[59]. TsOH monohydrate was dried by azeotropic distillation of a toluene solution. An equimolar solution of DMAP in warm toluene was then added to the flask and the two solutions were mixed thoroughly. The resulting suspension was cooled to room temperature (RT) and the solid collected by filtration. The crude product was purified by recrystallization from dry dichloroethane, yielding white crystals.

3.2.1 Techniques

^{1}H NMR analyses were performed on a *Bruker Avance III* 400 MHz spectrometer with a warm 5 mm TXI triple resonance detection probe in $CDCl_3$ with TMS as an internal standard, in Nuclear Magnetic Resonance Laboratory of Coimbra Chemistry Centre.

For MALDI-TOF-MS analysis, the sample was dissolved in THF at a concentration of 10 mg/mL. HABA and HCCA (0.05 M in THF) were used as matrix. The dried-droplet sample preparation technique was used to obtain 1/1 ratio (sample/matrix); an aliquot of 1 μL of each sample was directly spotted on the MTP AnchorChip TM 600/384 TF MALDI target, Bruker Daltonik (Bremen, Germany), and before the sample dry, 1 μL of matrix solution in THF was added and allowed to dry at RT, to permit matrix crystallization. External mass calibration was performed with a peptide calibration standard (PSCII) for the range 700-3000 (9 mass calibration points); 0.5 μL of the calibration solution and matrix previously mixed in an eppendorf tube (1/2, v/v) were applied directly on the target and allowed to dry at RT. Mass spectrum was recorded using an *Autoflex III smartbeam1 MALDI-TOF mass spectrometer Bruker Daltonik* operating in the linear mode. Ions were formed upon irradiation by a smartbeam1 laser using a frequency of 200 Hz. The mass spectrum was produced by averaging 2500 laser shots collected across the whole sample spot surface by screening in the range m/z 750-3000. The laser irradiance was set to 35-40% (relative scale 0-100) arbitrary units according to the corresponding threshold required for the applied matrix systems. The MALDI-TOF-MS data was obtained by Dra. Paula Álvarez Chaver at Unidad de Espectrometria de Masas do Servizo de Determinación Estructural, Proteómica e Xenómica, Centro de Apoio Científico e Tecnolóxico á Investigación (CACTI), Universidade de Vigo (Spain).

ATR-FTIR analyses were carried out on a *JASCO FT/IR - 4200* spectrometer at RT for the range 4000-500 cm^{-1}, using 64 scans and a 4 cm^{-1} spacial resolution.

3.2.2 Computational procedures

NMR spectra processing and analysis were carried out using *MestReNova* software. *CS ChemDraw* was utilized as drawing tool for chemical structures and *GraphPad Prism* was employed in analysis and graph of ATR-FTIR and MALDI-TOF-MS data.

3.3 Synthesis strategies

3.3.1 Double-stage convergent growth approach

The general procedures, chemical shifts (in *ppm*) and synthetic reactions schemes are presented below.

Synthesis of isopropylidene-2,2-bis(methoxy)propionic acid [1]

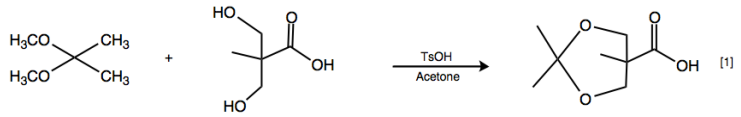

Figure 3.1: Isopropylidene-2,2-bis(methoxy)propionic acid synthesis reaction.

bis-MPA hydroxyl groups were protected to afford acetonide group by reacting bis-MPA (10.03 g, 74.77 mmol) with 2,2-dimethoxypropane (13.8 mL, 111.83 mmol) in distilled acetone (50 mL), catalyzed by TsOH anhydrous (0.71 g, 4.12 mmol). The reaction was stirred for 3 h at RT under N_2 atmosphere and the catalyst was neutralized by adding an equimolar solution of distilled triethylamine (0.41 g, 4.12 mmol). The solvent was evaporated, the residue was dissolved in CH_2Cl_2 and extracted with two portions of distilled water. The organic phase was dried with Na_2SO_4 anhydrous, filtered and the solvent evaporated to afford [1] as a white powder (6.77 g, 60%). ^{1}H NMR ($CDCl_3$): δ 1.20 (s, 3H, $-CH_3$), 1.43 (s, 3H, $-CH_3$), 1.46 (s, 3H, $-CH_3$), 3.68 (d, 2H, $-CH_2O$), 4.16 (d, 2H, $-CH_2O$).

Synthesis of benzyl-2,2-bis(methylol)propionate [2]

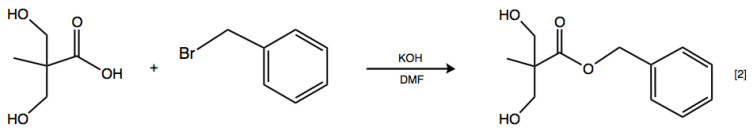

Figure 3.2: Benzyl-2,2-bis(methylol)propionate synthesis reaction.

bis-MPA (9.01 g, 67.71 mmol) and KOH (4.34 g, 77.35 mmol) were dissolved in 50 mL of DMF and the potassium salt was allowed to form at 100 °C for 1 h. Benzyl bromide (13.81 g, 80.74 mmol) was then added to the mixture. The reaction was stirred (800 rpm) for 15 h and then the solvent was evaporated off. The residue was dissolved in CH_2Cl_2 ($\sim$ 200 mL), extracted with three portions of distilled water, dried and the solvent was evaporated. The viscous oil obtained was recrystallized from CH_2Cl_2/hexane to give [2] as white crystals (9.31 g, 61%). ^{1}H NMR ($CDCl_3$): δ 1.08 (s, 3H, $-CH_3$), 3.75 (d, 2H, $-CH_2OH$), 3.94 (d, 2H, $-CH_2OH$), 5.21 (s, 2H, $-CH_2Ar$), 7.36 (m, 5H, ArH).

Synthesis of [G-2] dendron [3] and general esterification procedure

All esterification reactions were performed in distilled CH_2Cl_2 under Ar atmosphere at RT by DCC coupling, using DPTS as catalyst.

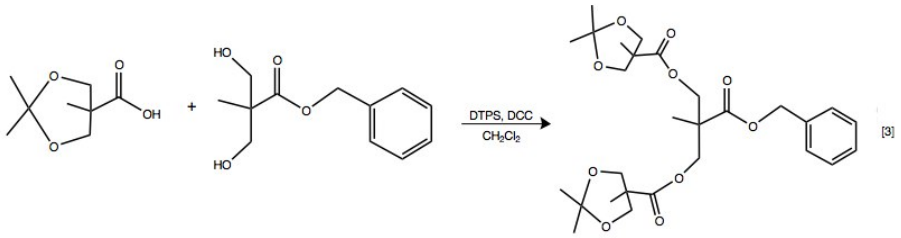

Figure 3.3: [G-2] dendron synthesis reaction.

[1] (3.26 g, 18.70 mmol), [2] (2.01 g, 8.96 mmol) and DPTS (1.05 g, 3.57 mmol) were dissolved in 30 mL of distilled CH_2Cl_2 and the reaction flask was flushed with Ar. DCC (4.61 g, 22.34 mmol) (in CH_2Cl_2) was then added and the reaction mixture was stirred overnight at RT under Ar atmosphere. After reaction completion, the DCC-urea byproduct was filtered off in a glass filter (with celite) and the residue was extracted with three portions of distilled water, dried and concentrated. The crude product was purified by liquid column chromatography on silica gel, eluting with hexane and gradually increasing to 50:50 EtOAc:hexane, to give [3] as a colorless viscous oil (2.99 g, 79%). ^{1}H NMR ($CDCl_3$): δ 1.10 (s, 6H, $-CH_3$), 1.30 (s, 3H, $-CH_3$), 1.34 (s, 6H, $-CH_3$), 1.41 (s, 6H, $-CH_3$), 3.56 (d, 4H, $-CH_2O$), 4.09 (d, 4H, $-CH_2O$), 4.34 (s, 4H, $-CH_2C$), 5.16 (s, 2H, $-CH_2Ar$), 7.34 (m, 5H, ArH).

General procedure for removal of benzyl ester group [4]

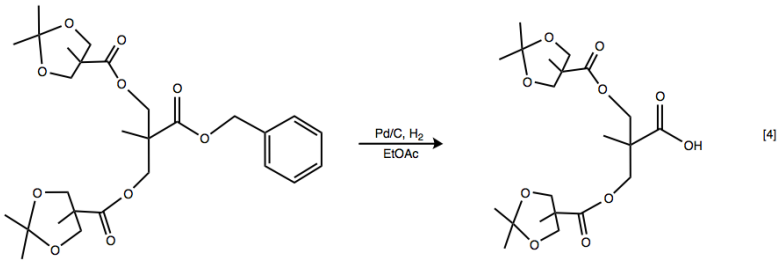

Figure 3.4: [G-2] dendron deprotection reaction of benzyl ester group.

The benzyl ester group was selectivity removed by catalytic hydrogenolysis performed at atmospheric pressure using Pd/C as catalyst. [3] (3.00 g, 5.59 mmol) was dissolved in EtOAc (25 mL) and 0.30 g of Pd/C (10%) was added to the solution. The flask was evacuated from air and filled with H_2 and the reaction was stirred for 24 h at RT. The catalyst was filtered off (with celite) and the solvent was evaporated to give [4] as a colorless viscous oil (2.29 g, 92%). ^{1}H NMR ($CDCl_3$): δ 1.16 (s, 6H, $-CH_3$), 1.32 (s, 3H, $-CH_3$), 1.36 (s, 6H, $-CH_3$), 1.42 (s, 6H, $-CH_3$), 3.62 (d, 4H, $-CH_2O$), 4.15 (d, 4H, $-CH_2O$), 4.35 (s, 4H, $-CH_2C$).

General procedure for removal of acetonide protective groups [5]

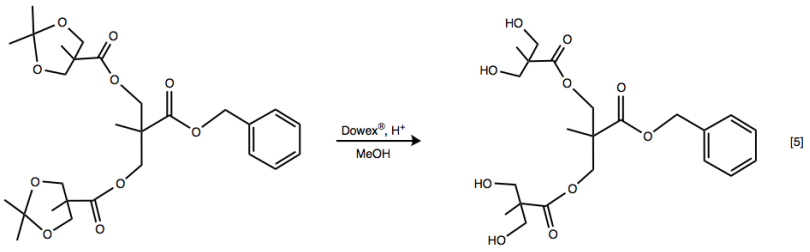

Figure 3.5: [G-2] dendron deprotection reaction of acetonide groups.

[3] (4.00 g, 7.45 mmol) was dissolved in 50 mL of methanol and approximately one teaspoon of Dowex H^+ resin was added to the solution. The reaction was stirred for 12 h under mild conditions and monitored by thin-layer chromatography (TLC). After reaction completion, the acidic Dowex

resin was filtered off in a glass filter (with celite) and the methanol was evaporated. To effectively isolated it, the crude product was then dissolved in EtOAc and washed with two portions of brine. The organic phase was dried with Na_2SO_4 anhydrous and concentrated to afford [5] as a powder (1,87 g, 55%). ^{1}H NMR ($CDCl_3$): δ 0.98 (s, 6H, $-CH_3$), 1.32 (s, 3H, $-CH_3$), 3.64-3.81 (m, 8H, $-CH_2OH$), 4.29 (d, 2H, $-CH_2C$), 4.44 (d, 2H, $-CH_2C$), 5.18 (s, 2H, $-CH_2Ar$), 7.35 (m, 5H, ArH).

Synthesis of [G-4] dendron [6]

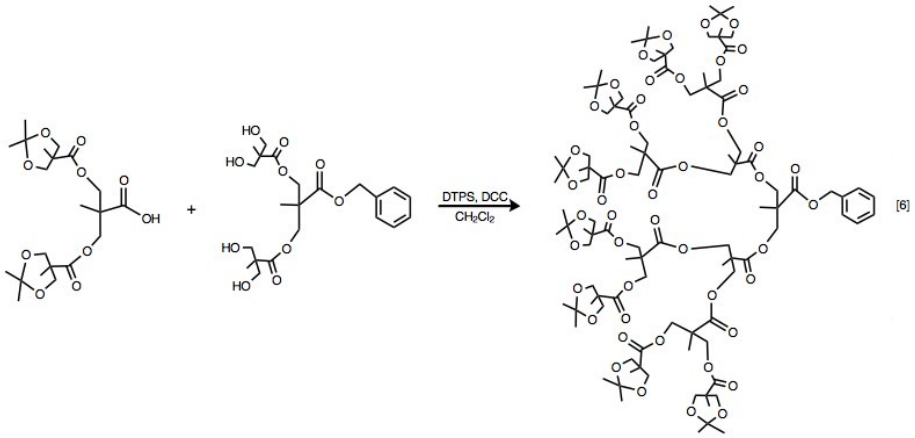

Figure 3.6: [G-4] dendron synthesis reaction.

The fourth generation dendron was attained by a coupling reaction according to the esterification general procedure. [4] (1.18 g, 2.64 mmol), [5] (207 mg, 0.45 mmol) and DPTS (515 mg, 1.75 mmol) were dissolved in 15 mL of distilled CH_2Cl_2 and flushed with Ar. DCC (589 mg, 2.85 mmol) was then added and the reaction mixture was stirred for 48 h at RT under Ar atmosphere. After reaction completion, the DCC-urea byproduct was filtered off in a glass filter and the residue was extracted with two portions of water; it was dried (with Na_2SO_4 anhydrous) and concentrated. The crude product was purified by liquid column chromatography on silica gel, eluting with hexane and gradually increasing to 80:20 EtOAc:hexane, to give [6] as a colorless viscous oil (891 mg, 91%). ^{1}H NMR ($CDCl_3$): δ 1.14 (s, 24H, $-CH_3$), 1.16 (s, 6H, $-CH_3$), 1.26 (s, 12H, $-CH_3$), 1.29 (s, 3H, $-CH_3$), 1.35 (s, 24H, $-CH_3$), 1.41 (s, 24H, $-CH_3$), 3.60 (d, 16H, $-CH_2O$), 4.13 (d, 16H, $-CH_2O$), 4.20-4.33 (m, 28H, $-CH_2C$), 5.16 (s, 2H, $-CH_2Ar$), 7.35 (m, 5H, ArH).

Removal of the benzyl ester group of [G-4] dendron [7]

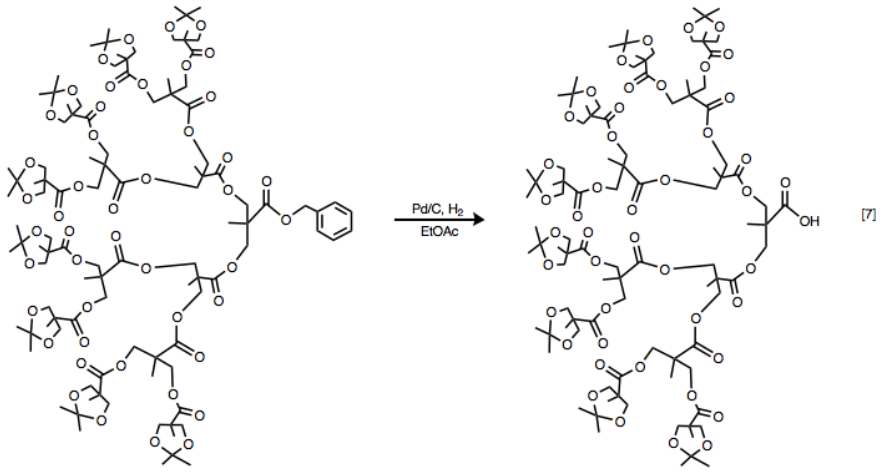

Figure 3.7: [G-4] dendron deprotection reaction of benzyl ester group.

The benzyl ester group was selectivity removed by catalytic hydrogenolysis according to the general procedure. [6] (3.09 g, 1.42 mmol) was dissolved in EtOAc (50 mL) and 0.31 g of Pd/C (10%) was added to the solution. The reaction mixture was stirred for 24 h at 30 °C at 10 atm. The catalyst was filtered off (with celite) and the solvent was evaporated to give [7] as a colorless viscous oil (2.1 g, 71%). ^{1}H NMR ($CDCl_3$): δ 1.14 (s, 24H, $-CH_3$), 1.26 (s, 18H, $-CH_3$), 1.28 (s, 3H, $-CH_3$), 1.35 (s, 24H, $-CH_3$), 1.42 (s, 24H, $-CH_3$), 3.61 (d, 16H, $-CH_2O$), 4.14 (d, 16H, $-CH_2O$), 4.20-4.33 (m, 28H, $-CH_2C$).

Alkyne functionalization of [G-4] dendron

An overview of the reactions carried out to accomplish the alkyne functionalization of the core of the dendrons is shown in Table 3.1.

General procedure: [7] and 3-butyn-1-ol were dissolved in distilled CH_2Cl_2 and the flask was flushed with N_2. The reaction mixture was cooled in an ice bath and a solution of DCC (in CH_2Cl_2) was added while stirring. A solution of DMAP was added dropwise under N_2 atmosphere and the mixture was stirred in the cooling bath for 1 h and then for 24 h at RT. The solution was filtered off with a glass filter, quenched with water and washed with a NaOH (5%) solution. The organic phase was dried with Na_2SO_4 anhydrous

and the solvent was evaporated. The crude product was purified by liquid column chromatography (on silica gel and eluting with 20:80 EtOAc:hexane) to afford a viscous oil.

3.3.2 Dendron growth *via* anhydride chemistry

Synthesis of isopropylidene-2,2-bis(methoxy)propionic acid anhydride [A1]

Figure 3.8: Isopropylidene-2,2-bis(methoxy)propionic acid anhydride synthesis reaction.

[1] (4.80 g, 27.6 mmol) was dissolved in 50 mL of distilled CH_2Cl_2 and flushed with N_2. DCC (2.85 g, 13.8 mmol) was added to the mixture and the reaction was continued for 15 h at RT under N_2 atmosphere. After reaction completion, DCC-urea byproduct was filtered off in a glass filter (2x) and the solvent was evaporated. The residue was dried under vacuum to obtain [A1] as a viscous oil (4.56 g, 95%). ^{1}H NMR ($CDCl_3$): δ 1.24 (s, 6H, $-CH_3$), 1.40 (s, 6H, $-CH_3$), 1.44 (s, 6H, $-CH_3$), 3.67 (d, 4H, $-CH_2O$), 4.20 (d, 4H, $-CH_2O$).

General procedure for the anhydride coupling reaction (synthesis of [A2])

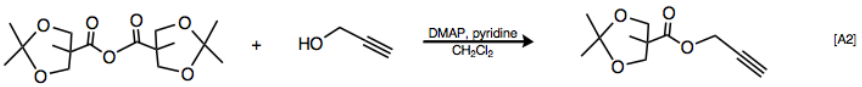

Figure 3.9: Anhydride coupling synthetic reaction.

Propargyl alcohol (261 mg, 4.66 mmol), DMAP (85 mg, 0.70 mmol) and pyridine (1.11 g, 14.01 mmol) were dissolved in 20 mL of distilled CH_2Cl_2 and flushed with N_2. [A1] (2.00 g, 6.05 mmol) was then added dropwise.

Table 3.1: [G-4] dendron alkyne functionalization attempts for different conditions.

Entry	**Dendron**	**Alkyne terminal**	**Catalysts**	**Solvent**	**t (h)**	**[7]/[alkyne terminal]/[catalyst1]/[catalyst2]**
1	[7]	Propargylamine	DMAP/DIC	CH_2Cl_2	24	1.0/3.0/0.5/1.2
2	[7]	Propargylamine	DPTS/DCC	CH_2Cl_2	48	1.0/3.0/0.5/1.2
3	[7]	Propargylamine	CDI	THF	24	1.0/5.0/2.0/0.0
4	[7]	4-Pentyn-1-ol	DPTS/DCC	CH_2Cl_2	48	1.0/3.0/0.5/1.2
5	[7]	3-Butyn-1-ol	DMAP/DCC	CH_2Cl_2	24	1.0/3.0/0.5/1.2
6	[7]	3-Butyn-1-ol	DMAP/EDC	CH_2Cl_2	40	1.0/4.0/2.0/2.0
7	[7]	3-Butyn-1-ol	DMAP/EDC	DMF	40	1.0/4.0/2.0/2.0

The mixture was stirred for 48 h at RT under N_2 atmosphere and monitored by TLC. The reaction was quenched with water (to remove excess of anhydride), washed with brine (2x) and the organic phase was dried with Na_2SO_4 anhydrous and concentrated. If necessary, the crude product was purified by liquid column chromatography on silica gel, eluting with hexane and gradually increasing to 80:20 EtOAc:hexane, to give [A2] as a colorless viscous oil (0.82 g, 64%). ^{1}H NMR ($CDCl_3$): δ 1.22 (s, 3H, $-CH_3$), 1.39 (s, 3H, $-CH_3$), 1.43 (s, 3H, $-CH_3$), 2.47 (t, 1H, $-C \equiv CH$), 3.65 (d, 2H, $-CH_2O$), 4.20 (d, 2H, $-CH_2O$), 4.74 (d, 2H, $-CH_2C \equiv CH$).

Removal of acetonide protective groups [A3]

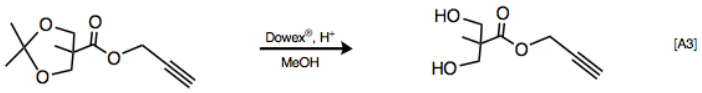

Figure 3.10: Deprotection reaction of acetonide groups of [A2].

[A2] was deprotected according to the general procedure for the removal of acetonide protective groups (71%). ^{1}H NMR ($CDCl_3$): δ 1.10 (s, 3H, $-CH_3$), 2.50 (t, 1H, $-C \equiv CH$), 3.73 (d, 2H, $-CH_2O$), 3.93 (d, 2H, $-CH_2O$), 4.77 (d, 2H, $-CH_2C \equiv CH$).

Synthesis of [G-2] dendron [A4]

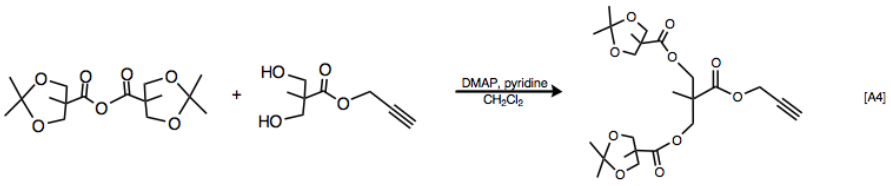

Figure 3.11: [G-2] dendron synthesis reaction.

General procedure for dendritic generation growth through anhydride coupling reaction: [A3] (580 mg, 3.36 mmol), DMAP (230 mg, 1.88 mmol) and pyridine (3.30 g, 41.77 mmol) were dissolved in 30 mL of distilled CH_2Cl_2 and flushed with N_2. [A1] (3.07 g, 9.28 mmol) was then added and the solution was stirred for 24 h at RT under N_2 atmosphere. The reaction was monitored by TLC until total completion. It was washed with a

solution of NaOH (10%) and the organic phase was dried, filtered, concentrated and purified by liquid column chromatography on silica gel, eluting with hexane and gradually increasing to 80:20 EtOAc:hexane, to give [A4] as a viscous oil (960 mg, 59%). ^{1}H NMR ($CDCl_3$): δ 1.16 (s, 6H, $-CH_3$), 1.32 (s, 3H, $-CH_3$), 1.36 (s, 6H, $-CH_3$), 1.42 (s, 6H, $-CH_3$), 2.48 (t, 1H, $-C \equiv CH$), 3.61 (d, 4H, $-CH_2O$), 4.14 (d, 4H, $-CH_2O$), 4.34 (s, 4H, $-CH_2C$), 4.72 (d, 2H, $-CH_2C \equiv CH$).

Removal of acetonide protective groups [A5]

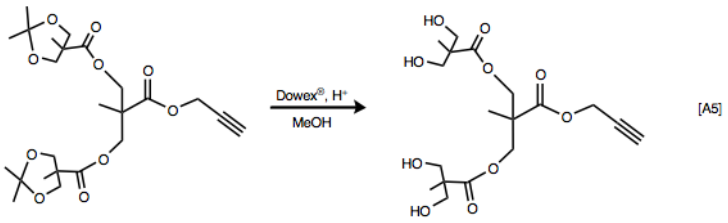

Figure 3.12: [G-2] dendron deprotection reaction of acetonide groups.

[A5] was obtained according to the general deprotection procedure of acetonide groups (previously reported) (56%). ^{1}H NMR ($CDCl_3$): δ 1.06 (s, 6H, $-CH_3$), 1.25 (s, 3H, $-CH_3$), 2.49 (t, 1H, $-C \equiv CH$), 3.70-3.88 (m, 8H, $-CH_2OH$), 4.32 (d, 2H, $-CH_2C$), 4.46 (d, 2H, $-CH_2C$), 4.75 (d, 2H, $-CH_2C \equiv CH$).

Synthesis of [G-4] dendron [A6]

[A5] (37.7 mg, 0.093 mmol), [4] (250 mg, 0.56 mmol) and DPTS (110 mg, 0.37 mmol) were dissolved in 20 mL of distilled CH_2Cl_2 and the flask was flushed with Ar. DCC (125 mg, 0.60 mmol) was added and the reaction mixture was stirred for 48 h at RT under Ar atmosphere. Reaction byproducts were filtered off and the organic phase was extracted with three portions of water, dried (with Na_2SO_4 anhydrous) and the solvent was evaporated. The crude product was then purified by liquid column chromatography on silica gel, eluting with hexane and gradually increasing the polarity to 80:20 EtOAc:hexane (148 mg, 75%). ^{1}H NMR ($CDCl_3$): δ 1.17 (s, 24H, $-CH_3$), 1.31 (s, 18H, $-CH_3$), 1.37 (s, 24H, $-CH_3$), 1.42 (s, 24H, $-CH_3$), 3.62 (d, 16H, $-CH_2O$), 4.16 (d, 16H, $-CH_2O$), 4.25-4.41 (m, 28H, $-CH_2C$), 4.74 ($-CH_2C \equiv CH$).

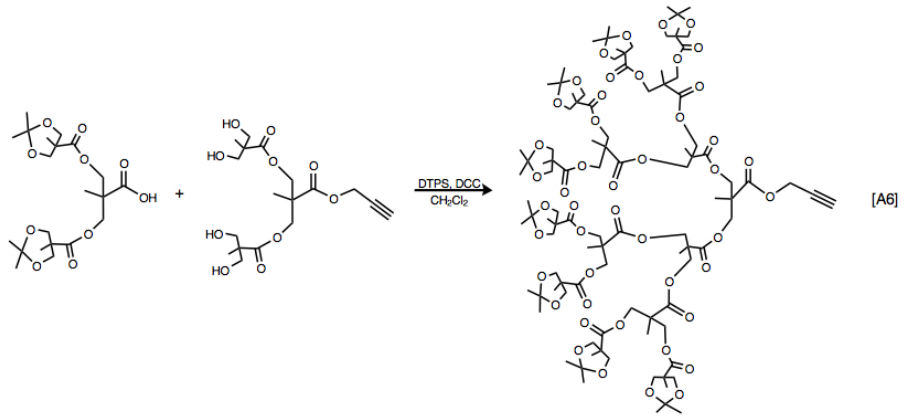

Figure 3.13: Esterification reaction scheme.

Synthesis of '2^{nd} generation' anhydride [D1]

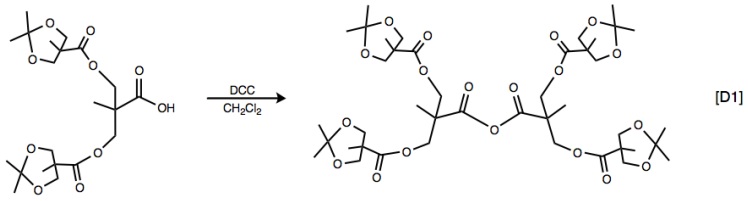

Figure 3.14: Anhydride synthesis reaction scheme.

[4] (2.10 g, 4.70 mmol) was dissolved in 20 mL of distilled CH_2Cl_2 and bubbled with N_2. DCC (0.49 g, 2.35 mmol) was then added to the mixture and the reaction was continued for 24 h at RT under N_2 atmosphere. After reaction completion, DCC-urea byproduct was filtered off and the solvent was evaporated (1.15 g, 55%). ^{1}H NMR ($CDCl_3$): δ 1.16 (s, 12H, $-CH_3$), 1.32 (s, 6H, $-CH_3$), 1.36 (s, 12H, $-CH_3$), 1.42 (s, 12H, $-CH_3$), 3.62 (d, 8H, $-CH_2O$), 4.16 (d, 8H, $-CH_2O$), 4.34 (m, 8H, $-CH_2C$).

Synthesis of [G-3] dendron through anhydride coupling reaction [D2]

[A3] (82.8 mg, 0.48 mmol), DMAP (15.3 mg, 0.12 mmol) and pyridine (322.7 mg, 4.08 mmol) were dissolved in distilled CH_2Cl_2 (20 mL) and flushed with N_2. [D1] (0.91 mg, 5.29 mmol) was then added and the

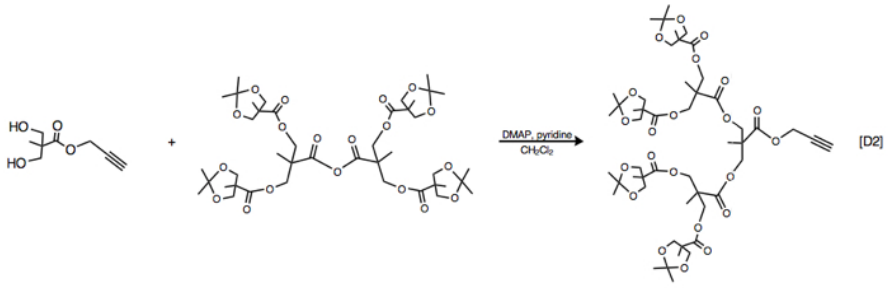

Figure 3.15: [G-3] dendron synthesis reaction.

solution was stirred for 24 h at RT under N_2 atmosphere. The reaction was monitored by TLC and then it was washed with distilled water (3x), dried and concentrated. The product was purified by liquid column chromatography on silica gel, eluting with 20:80 EtOAc:hexane and gradually increasing the polarity to 100% EtOAc (386 mg, 78%). ^{1}H NMR ($CDCl_3$): δ 1.08-1.16 (m, 12H, $-CH_3$), 1.28 (s, 6H, $-CH_3$), 1.31 (s, 3H, $-CH_3$), 1.36 (s, 12H, $-CH_3$), 1.43 (s, 12H, $-CH_3$), 2.45 (t, 1H, $-C \equiv CH$), 3.61 (d, 8H, $-CH_2O$), 4.16 (d, 8H, $-CH_2O$), 4.26-4.47 (m, 12H, $-CH_2C$), 4.74 ($-CH_2C \equiv CH$).

3.3.3 Alkyne functionalization of [1]

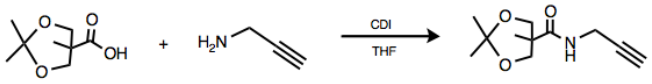

Figure 3.16: Synthesis reaction scheme.

[1] (1.74 g, 10.0 mmol) was dissolved in distilled THF (50 mL) and the flask was flushed with N_2. A solution of CDI (3.24 g, 20.0 mmol) was then added and the reaction was stirred for 4 h at 25 °C (in a water bath) under Ar atmosphere. Propargylamine (826 mg, 15.02 mmol) was then added and the resulting mixture was continued for 24 h. The solvent was evaporated and the residue was dissolved in CH_2Cl_2 ($\sim$ 50 mL) and washed with distilled water (2x), dried over Na_2SO_4 anhydrous, filtered and evaporated (1.27 g, 60%). ^{1}H NMR ($CDCl_3$): δ 1.25 (t, 3H, $-CH_3$), 2.24 (t, 1H), 3.98 (d, 2H, $-CH_2C$), 4.14 (d, 2H, $-CH_2C$).

3.3.4 Alkyne functionalization of PEG

Table 3.2 summarizes the reactions carried out to attain this objective.

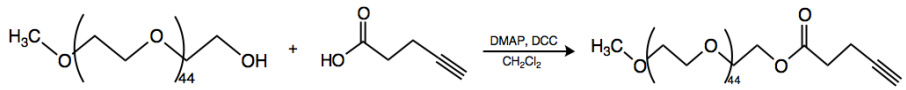

Figure 3.17: Synthesis reaction of terminal alkyne-functionalized PEG.

General procedure: Dry PEG_{2000} (4.32 g, 2.16 mmol), 4-pentynoic acid (0.25 g, 2.55 mmol) and DMAP (0.12 g, 0.98 mmol) were dissolved in 30 mL of distilled CH_2Cl_2 and the solution was cooled in an ice bath. The reaction flask was flushed with Ar and DCC (0.59 g, 2.86 mmol) was then added. The reaction mixture was kept in the ice bath for $\sim$ 10 min and was stirred for 15 h at RT under Ar atmosphere. After reaction completion, the DCC-urea byproduct was filtered off and the solution was precipitated into cold diethyl ether. The product was then filtered and dried under vacuum (to obtain a white powder) (2.95 g, 66%). ^{1}H NMR ($CDCl_3$): δ 1.99 (t, 1H, $-C \equiv CH$), 2.47-2.54 (m, 2H, $-CH_2C \equiv CH$), 2.56-2.62 (m, 2H, $-CH_2C$), 3.38 (s, 3H, $-CH_3$), 3.54-3.75 (m, 178H, $-CH_2$), 4.26 (t, 2H, $-CH_2O$).

3.3.5 'Click' reaction: PEG-PDMAEMA block copolymer synthesis attempts

After the synthesis of the alkyne-functionalized PEG, 'click' reactions were carried out in order to assemble a PEG-b-PDMAEMA copolymer. Table 3.3 shows the conditions of the reactions performed.

General procedure: In a vial were placed PDMAEMA-azide (653 mg, 0.081 mmol) and DMF (3 mL). A schlenk flask was charged with PEG-alkyne (204 mg, 0.098 mmol), CuBr (25.7 mg, 0.179 mmol), N,N,N',N",N"-pentamethyl-diethylenetriamine (PMDETA) (31.1 mg, 0.179 mmol) and DMF (4 mL). DMF was previously bubbled in N_2 during 15 min. The content of the vial was charged into the schlenk flask, deoxygenated with three freeze-pump-thaw cycles and purged with N_2. The reactor was placed in a pre-heated oil bath at 70 °C with stirring (700 rpm) during 48 h. The copolymer was dialyzed (in distilled water for 3 days) and freeze-dryied.

Table 3.2: PEG alkyne functionalization attempts for different conditions.

Entry	**Alkyne terminal**	**Catalysts**	**Solvent**	**t (h)**	**T (°C)**	**[PEG_{2000}]/[alkyne terminal]/[catalyst1]/[catalyst2]**
1	Propiolic acid	DMAP/DCC	CH_2Cl_2	24	RT	1.0/1.23/0.42/1.33
2	Propiolic acid	DPTS/DIC	CH_2Cl_2	24	RT	1.0/1.23/0.31/1.33
3	Propargyl bromide	NaH	THF	15	RT	1.0/5.0/10.0/0.0
4	Propargyl bromide	NaH	THF	15	60	1.0/5.0/10.0/0.0
5	Propargyl bromide	NaH	THF	24	60	1.0/7.35/10.3/0.0
6	4-Pentynoic acid	DMAP/DCC	CH_2Cl_2	15	RT	1.0/1.18/0.45/1.32

Table 3.3: 'Click' reactions attempts overview ([PEG-alkyne]/[PDMAEMA-azide]/[CuBr]/[PMDETA] 1.2/1.0/2.2/2.2 ratio)

Entry	$\mathbf{M}_{n(PEG-alkyne)}$ (g/mol)	$\mathbf{M}_{n(PDMAEMA-azide)}$ (g/mol)	**DMF** (mL)
1	2088.1	7886	8
2	2088.1	12812	7

PDMAEMA synthesis

PDMAEMA was synthetized by LRP:

1. Entry #1
   - Initiator: CHO-Br
   - Catalytic system: CuBr
   - Ligand: PMDETA
   - Solvent: THF
   - T: 60 °C
   - t: 4 h
   - [DMAEMA]/[CHO-Br]/[CuBr]/[PMDETA]: 45/1/1/1
   - $[monomer]_0$/[solvent] (v/v): 1/1
2. Entry #2
   - Initiator: EBiB
   - Catalytic system: Fe(0)/$CuBr_2$
   - Ligand: PMDETA
   - Solvents (v/v): isopropanol/H_2O (9/1)
   - T: 60 °C
   - t: 48 h
   - [DMAEMA]/EBiB]/[Fe(0)]/[$CuBr_2$]/[PMDETA]: 45/1/0.1/1/1
   - $[monomer]_0$/[solvent] (v/v): 1/1

PDMAEMA azidation reaction

General procedure: A schlenk flask was charged with EBiB-PDMAEMA and DMF (previously bubbled in N_2). Sodium azide (NaN_3) was then added to the mixture. The reactor was purged with N_2 and placed in a pre-heated oil bath at 60 °C with stirring during 48 h. The polymer was dialyzed and freeze-dryied.

4

Results Analysis

4.1 Double-stage convergent growth approach

The synthetic route adopted to construct an aliphatic polyester monodendron based on bis-MPA was a double-stage convergent growth approach, developed by Fréchet (Figure 2.6)[32]. This method allow the synthesis of the [G-4] dendron in six steps, reducing the number of synthetic steps when compared to a strict convergent growth. The synthesis is essentially straightforward and the aliphatic ester backbone renders dendrons suitable for biomedical applications.

First, bis-MPA moiety was protected to afford an acetonide group ([1]). In the next step, the acid group in bis-MPA was protected by a benzyl ester group by reaction of the potassium salt of bis-MPA with benzyl bromide ([2]). Chemical shifts of ^{1}H NMR spectrum at 5.21 and 7.36 ppm confirm the presence of the benzyl group. It is selectivity removed, in high yields, by catalytic hydrogenolysis without affecting the ester bonds of the dendron.

Esterification reactions were performed using DPTS as catalyst and DCC as the dehydration agent. Despite all the disadvantages of DCC, such as formation of N-acylurea, steric hindrance and decrease of yields, several bis-MPA based dendrimers reported have been successfully synthesized in this fashion. Moreover, purification process by column chromatography (on silica gel) was necessary after each esterification reaction.

The acetonide groups could be deprotected in the presence of an acidic Dowex resin, confirmed by the disappearance of two singlets related to the methyl groups ([5]).

The fourth generation dendron ([6]) was then obtained in a final coupling step between dendrons [4] and [5], according to the general procedure described previously.

NMR spectra of different dendron generations ([1] to [6]) may be seen in

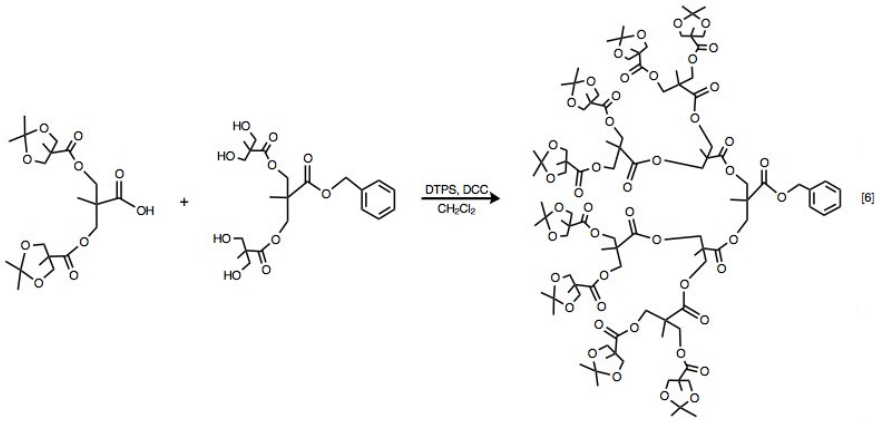

Figure 4.1: [6] synthesis reaction.

Appendix A. Successful formation of each generation of dendrons was confirmed by the peak integration ratio and the results obtained are discussed. It can be seen that resonances from the methyl groups are well separated up to the second generation but in the fourth generation become almost coincident.

Benzyl ester group of compound [6] was then deprotected by hydrogenolysis to give dendron [7], which core can be functionalized with an alkyne moiety. In this deprotection step, difficulties were encountered to obtain a significant cleavage. In this way, several attempts were conducted until optimal conditions were attained (stirring, P_{H_2} = 10 atm, T = 30 °C, t = 24 h). Higher pressure was tested and it seems that acetonide groups were affected and degraded.

^{1}H NMR, ATR-FTIR, MALDI-TOF-MS characterization techniques were applied to assess structural condition of dendron [7].

Figure 4.2 depicts the ^{1}H NMR spectrum of [7] and confirms the success of this reaction through the disappearance of the resonance signals at 5.16 ($-CH_2Ar$) and 7.35 (ArH) ppm.

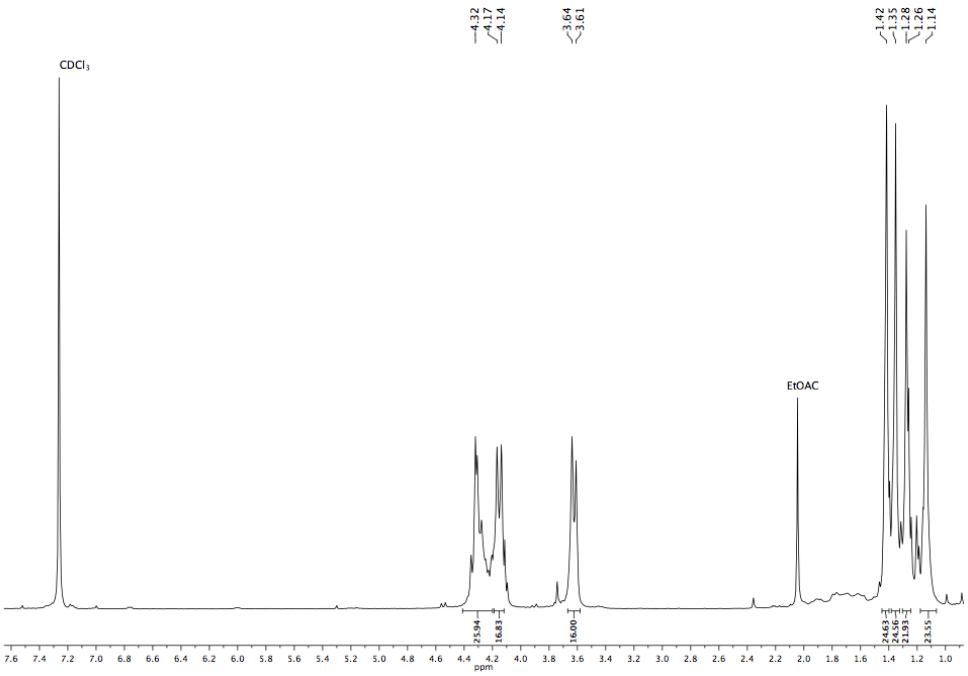

Figure 4.2: ^{1}H NMR spectrum of [7].

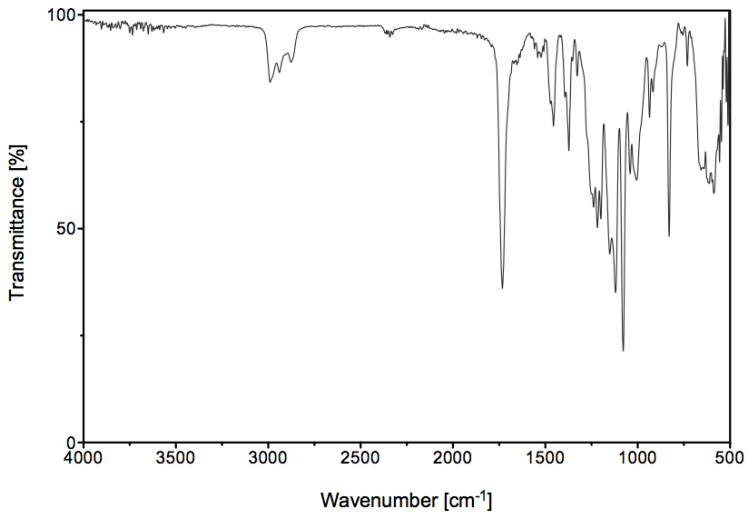

Figure 4.3: ATR-FTIR transmittance spectrum of [7].

ATR-FTIR analysis was also performed to assess whether carboxylic acid was affected. The spectrum obtained (Figure 4.3) reveals the absence of the

carboxylic group characteristic absorption peak. Thus, MALDI-TOF-MS analysis of [7] was conducted in order to assess the integrity of the dendron.

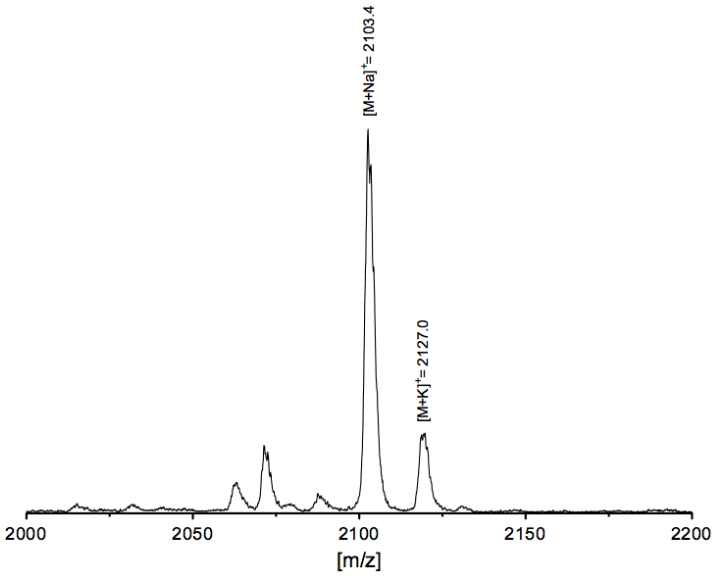

Figure 4.4: Enlargement of the MALDI-TOF-MS in the linear mode from m/z 2000 to 2200 of dendron [7] with theoretical molecular weight of [M+Na^+] = 2103.25 Da.

MALDI-TOF-MS was employed for the determination of molecular weight of the dendron. The results are in agreement with the calculated values, as shown in Figure 4.4, corroborating the presence of the carboxylic group, unlike suggested by FT-IR technique.

Alkyne functionalization of [G-4] dendron

The next step in this work was the alkyne functionalization of the core of the dendron [7]. For that reason, several attempts for different conditions (Table 3.1) were conducted and NMR spectra of each reaction performed is presented in Appendix A.

For entry #1 to #3, it was expected to find acetylene resonances of the propargylamine around 2.24 and 3.4 ppm and for the three systems tested it was found that the reactions were incomplete (confirmed by peak integration and by the absence of the peak at 3.4 ppm).

The low reactivity of propargylamine could be one of the aspects of failure of these reactions. In this way, a new alkyne terminal (4-pentyn-1-ol) was tested, using DPTS and DCC as catalysts.

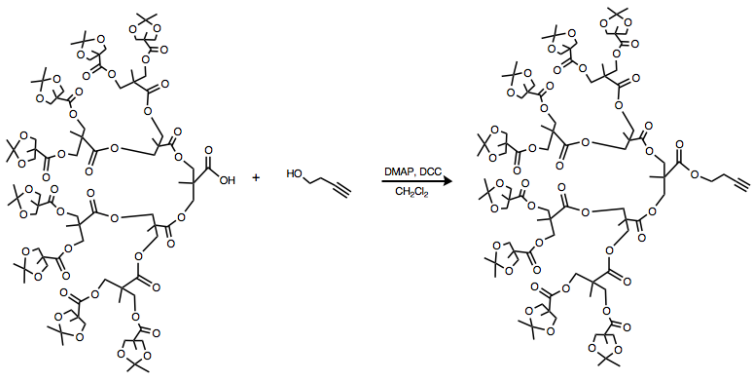

Figure 4.5: Example of an alkyne functionalization reaction scheme (entry #5).

Entry #4 NMR spectrum shows a peak at 2.1 ppm that seems to correspond to acetylene group, but with an integration ratio value below the expected. 1.8 and 3.7 ppm characteristic resonances reveal no noticeable signals since dendron has predominant signals in this region that may overlap. Resonance at 2.4 ppm is also absence.

Novel attempts (entry #5 to #7) were performed, in CH_2Cl_2 and DMF, using DMAP/DCC or DMAP/EDC as catalysts. Any of the three reactions reached total completion since only a peak around 2.56 ppm (related to the signal of $-CH_2C \equiv CH$) is present and resonances at 2.1 ($-C \equiv CH$) and 3.7 ($-CH_2-$) ppm are absent in the spectra.

In this way, the initial objective of alkyne functionalization of the core of the dendron wasn't accomplished.

4.2 Anhydride route

Since the reactions performed according to the previous approach weren't unsuccessful, a novel synthetic route to construct aliphatic polyester dendrons was carried out based on the dendritic generation growth through anhydride coupling reactions[60].This approach has several advantages such as short reaction time, facile workup, low-temperature esterification and higher reactivity when compared to the carboxylic acid.

Anhydride synthesis ([A1]) (in high yields) provide easy access to the alkyne terminal by condensation with the appropriate alcohol. [G-1] dendron ([A2]) was constructed with an acetylene group at the focal point and the success of the reaction was verified by ^{1}H NMR (which spectrum is presented

in Appendix B).

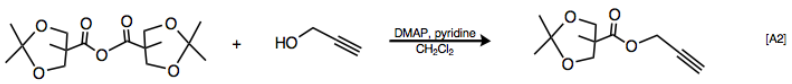

Figure 4.6: [A2] synthesis reaction.

Dendritic generation growth up to second generation continued through the removal of the acetonide group ([A3]) and subsequent acylation with the anhydride ([A4]).

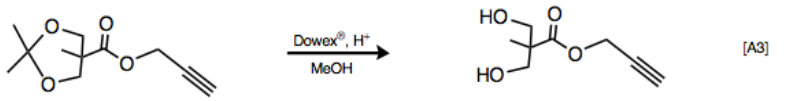

Figure 4.7: [A3] synthesis reaction.

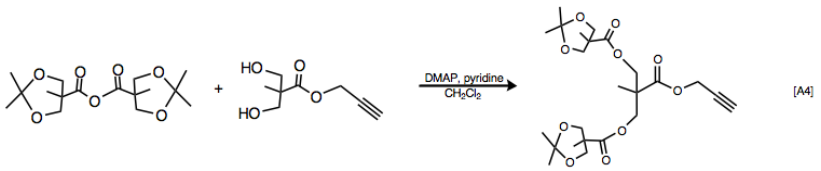

Figure 4.8: [A4] synthesis reaction.

The resulting [A4] dendron is rendered reactive by deprotection of the surface methylene groups.

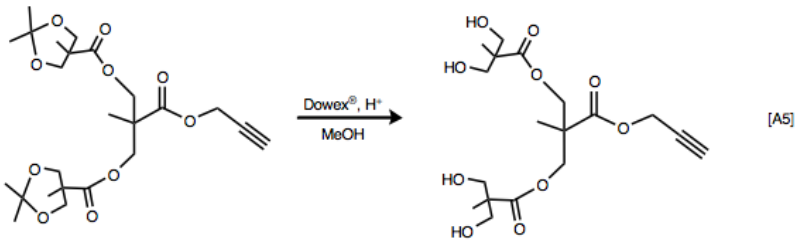

Figure 4.9: [A5] synthesis reaction.

At this point, a new approach was carried out based on the reaction of the dendron [4] with the dendron [A5]. With this esterification reaction, a [G-4] dendron can be designed faster and with less purification steps when compared to traditional acylation reactions with the anhydride.
Dendron [A6] was characterized by ^{1}H NMR and ATR-FTIR and the results obtained are presented below.

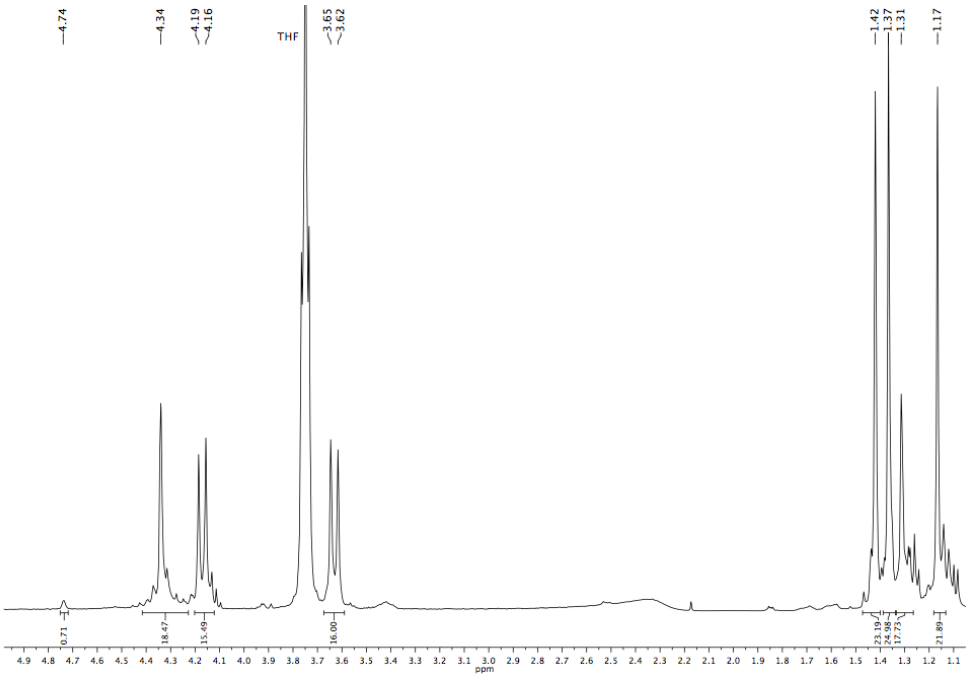

Figure 4.10: ^{1}H NMR spectrum of [A6].

Unexpectedly, the resonance at 2.48 ppm corresponding to the $-C \equiv CH$ group is absent and a decrease in the integration ratio of the peak at 4.74 ppm related to $-CH_2C \equiv CH$ group is verified. Although esterification reaction has occurred (since methylene resonances at 1.17, 1.31, 1.37 and 1.42 ppm are depicted), the conditions of operation could be one of the reasons for the eventually degradation of the alkyne terminal, preventing a 'click' reaction. Formation of micellar aggregates could also be a hypothesis for the non-detection of the alkyne terminal in the NMR spectrum.

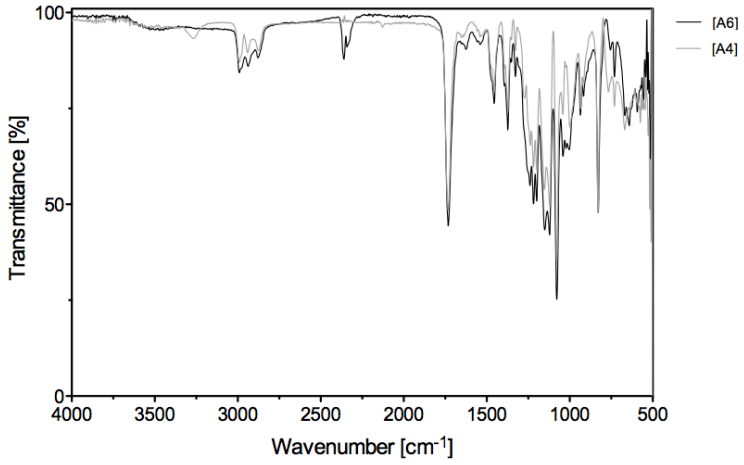

Figure 4.11: ATR-FTIR transmittance spectra of [A4] and [A6].

FT-IR spectrum of [A6] corroborates the previous conclusion due to the absence of acetylene characteristic absorption peaks around 3200 and 2100 cm^{-1} (corresponding to the alkyne terminal).

'2^{nd} generation' anhydride synthesis

With the same aim of shorten [G-4] dendron synthesis time and purification steps (and have knowledge of its high reactivity), we developed for the first time a 'second generation' anhydride, which was characterized by ^{1}H NMR and ATR-FTIR, confirming the success of the reaction.

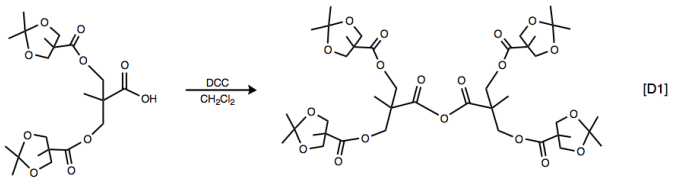

Figure 4.12: Anhydride synthesis reaction scheme.

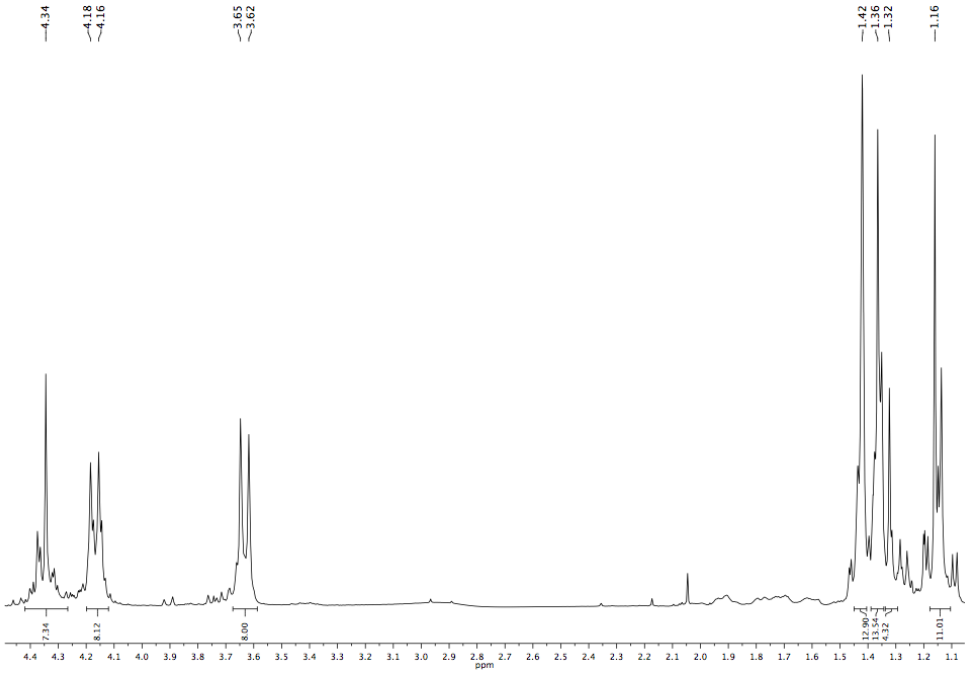

Figure 4.13: ^{1}H NMR spectrum of [D1].

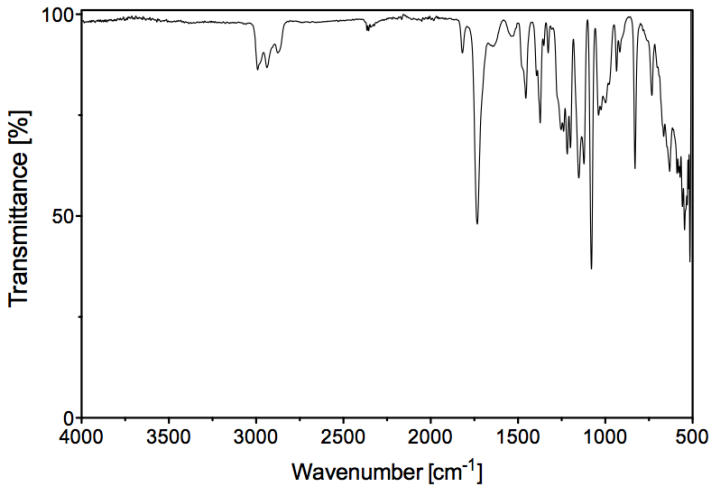

Figure 4.14: ATR-FTIR transmittance spectrum of [D1].

Next, an anhydride coupling reaction between anhydride [D1] and dendron [A3] was performed to afford a [G-3] dendron. The acylation reaction

was carried out according to the procedure described previously, but difficulties were encountered in the purification step. It was necessary to use a chromatography solvent of relative high polarity of 100% EtOAc to collect the compound [D2].

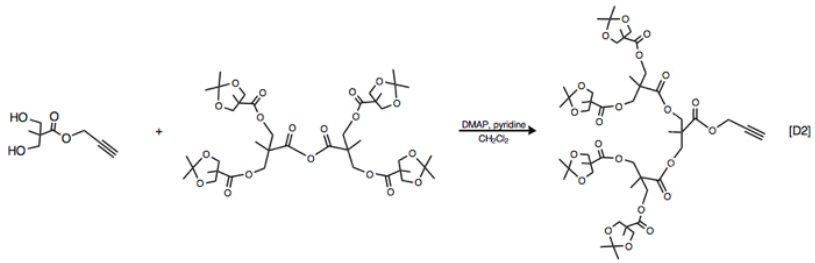

Figure 4.15: [D2] synthesis reaction.

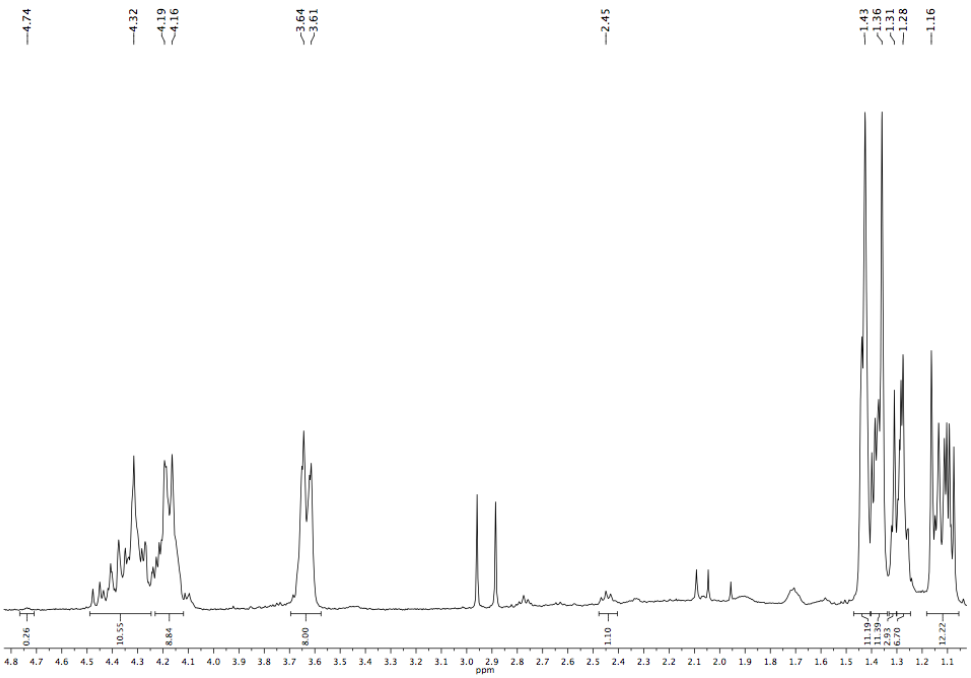

Figure 4.16: ^{1}H NMR spectrum of [D2].

^{1}H NMR spectrum of [D2] shows that acylation reaction was successfully performed but the signal of $-CH_2C \equiv CH$ group at 4.74 ppm, exhibits an integration ratio below the expected, although the acetylene resonance (at 2.45 ppm) wasn't affected.

4.3 Alkyne functionalization of [1]

An attempt to functionalize [1] with an alkyne terminal was also carried out (Figure 4.17).

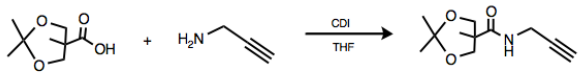

Figure 4.17: Synthesis reaction scheme.

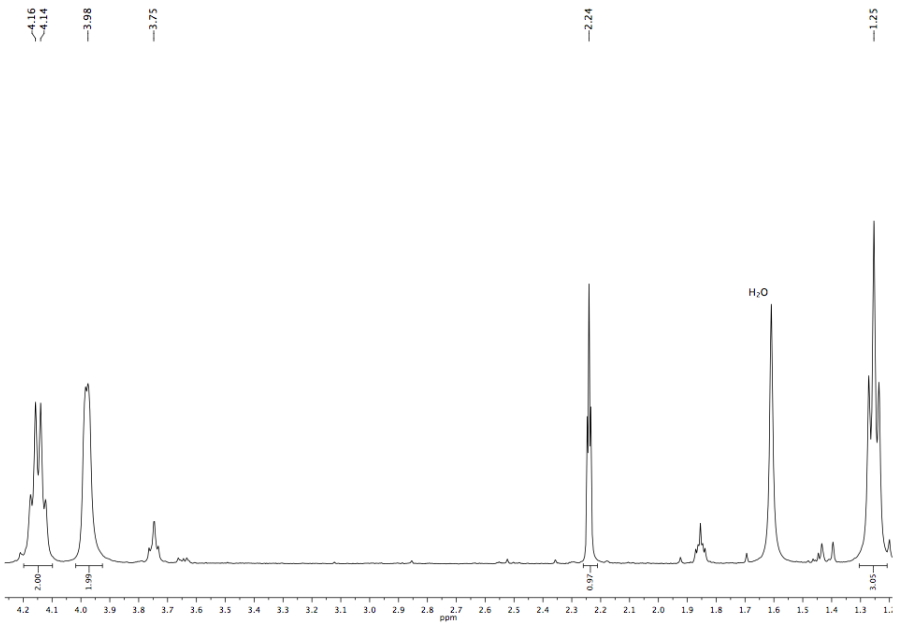

Figure 4.18: ^{1}H NMR spectrum of [1] alkyne functionalization reaction.

The ^{1}H NMR spectrum express the presence of acetylene resonance at 2.24 ppm but it also shows the absence of the peak referring to $-CH_2C \equiv CH$ group ($\sim$ 3.4 ppm). It can also be seen that acetonide group were affected and degraded.

ATR-FTIR spectrum shows an absorption peak around 3100 cm^{-1} with lower intensity when compared to compound [1], and a peak around 3300 cm^{-1}.

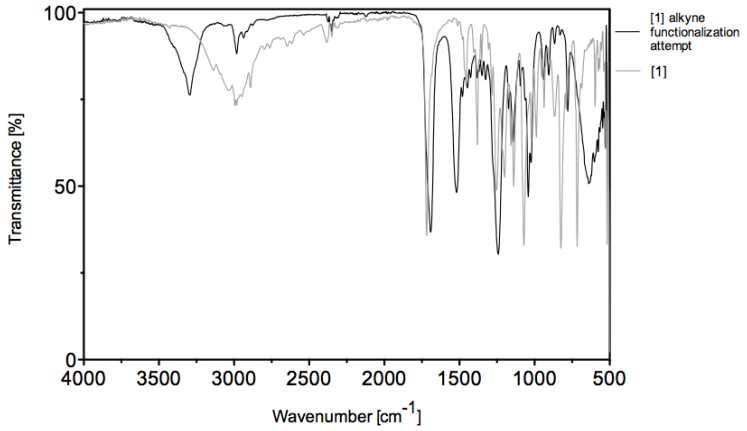

Figure 4.19: ATR-FTIR transmittance spectrum of [1] alkyne functionalization reaction.

4.4 Alkyne functionalization of PEG

Terminal alkyne functionalization of mono functional PEG (Mn $\sim$ 2000) was accomplish, following the general procedure described previously [61].

^{1}H NMR and ATR-FTIR spectra of the reactions performed are presented in Appendix C. After spectra analysis, it is concluded that attempts (Table 3.2), until entry #6, weren't successful, although NMR spectrum of reaction #5 shows resonances at 2.44 and 3.82 ppm that correspond to the chemical shifts of the alkyne terminal, but with an integration ratio below the expected.

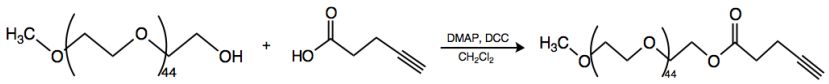

Figure 4.20: Synthesis reaction scheme of alkyne-functionalized PEG.

Figure 4.21 depicts the NMR spectrum of the alkyne-functionalized PEG. The appearance of a doublet at 2.51 and 2.59 ppm and a triplet at 1.99 ppm confirms the presence of the alkyne group in the backbone of the PEG.

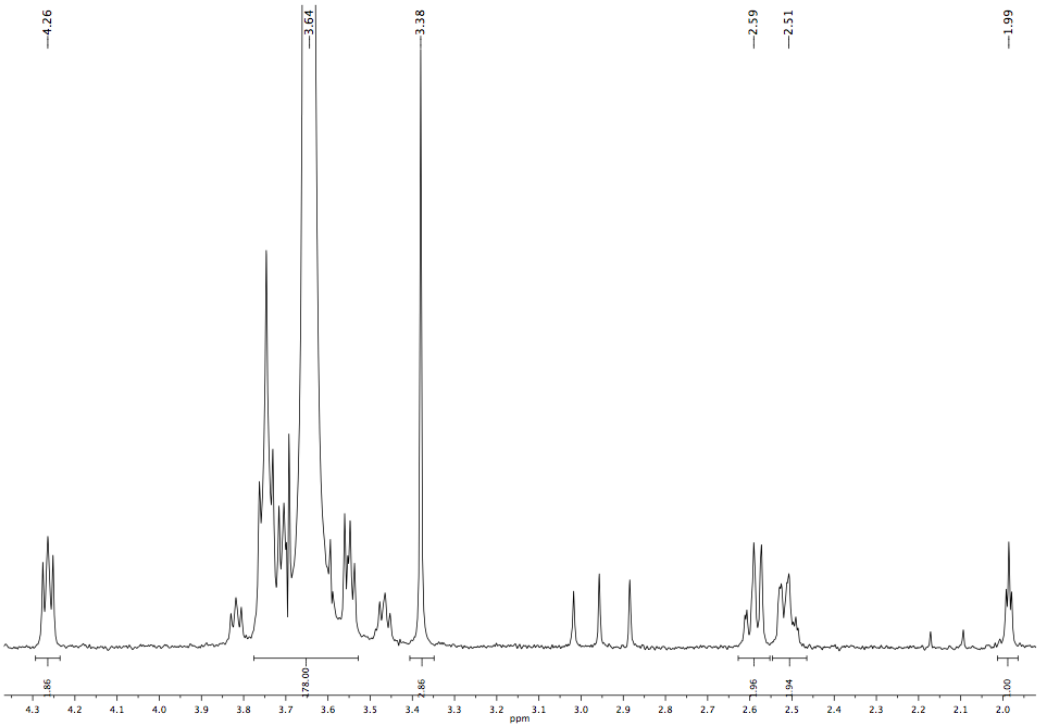

Figure 4.21: ^{1}H NMR spectrum of PEG-alkyne.

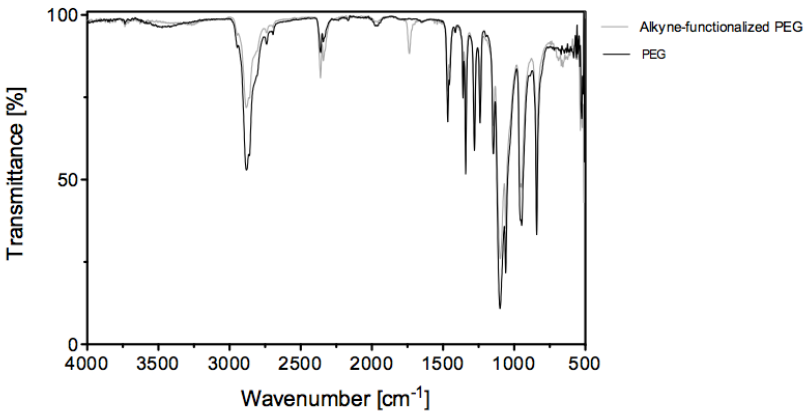

Figure 4.22: ATR-FTIR transmittance spectra of PEG and PEG-alkyne.

The appearance of peaks around 1720 and 3200 cm^{-1}, in the FT-IR spectrum, suggest the presence of a ester bond in the molecule (carbonyl group) and the alkynyl C-H stretch, respectively.

'Click' chemistry

After the synthesis of the alkyne-functionalized PEG, 'click' reactions were carried out in order to assemble a PEG-*b*-PDMAEMA copolymer. Later, it was find out that bromide terminals of PDMAEMA were affected, preventing an effective 'click' reaction.

5

Conclusion

Designing dendritic polymers is a challenging combination of organic and polymer chemistry and there are still problems that must be overcome to efficiently apply them to medical and pharmaceutical fields. From a theoretical point-of-view, dendrons and dendrimers exhibit attractive properties which make them ideal carriers for DDS (as previously referred). However, their synthesis methodology is a laborious multi-step route that present several problems.

Use of DCC as a neat reagent, which forms urea byproducts in each esterification reaction. In this way, the only approach to effectively purify them is through column chromatography processes. This time-consuming task is controlled by TLC (which sometimes makes it of difficult evaluation), requires an optimal polarity solvents balance to efficiently remove excess of reagents and often presents a low final yield.

Several attempts to deprotect selectively the benzyl group of the [G-4] dendron were performed due to the necessity of fine tuning of the optimal conditions to perform the catalytic hydrogenolysis.

Several alkyne functionalization reactions of the [G-4] dendron were carried out for different conditions. Different catalysts were tested, firstly, propargylamine, but due to its low reactivity, other alkyne terminals, such as 3-butyn-1-ol and 4-pentyn-1-ol, were used, as well as different solvents, but without success.

Alkyne terminal identification by NMR and FT-IR is also a arduous task due to the low integration ratio of this group. We also verified that alkyne terminal was affected during the esterification and acylation reactions performed.

We can conclude that for higher dendron generations, access to the core molecule is very difficult, probably, due to the restricted steric accessibility controlled by the highly branched architecture (sterically hindered surface difficults addition of new molecules). In this sense, other route (via anhy-

dride) was carried out, since it is more reactive, and a [G-2] dendron alkyne functionalized was accomplished in this fashion.

Low reactivity of propiolic acid and propargyl bromide could also influenced the unsuccessful alkyne functionalization reactions of PEG.

5.1 Future work

In the future, new catalytic systems could also be tested to attempt the alkyne functionalization of the [G-4] dendron and fine tuning of the optimal conditions to perform esterification and acylation reactions, in order to avoid acetylene group degradation, could be explored. Dendron growth *via* anhydride can be an alternative to the first methodology, as well as, attempt to functionalize dendrons of lower generations (using 3-butyn-1-ol instead of propagylamine). Functionalization of the alkyne terminal with a fluorescent molecule to identify, in a facile way, the success of the reaction might be also an alternative.

Bibliography

[1] J. F. Coelho, P. C. Ferreira, P. Alves, R. Cordeiro, A. C. Fonseca, J. R. Góis, and M. H. Gil. *EPMA Journal*, 1:164–210, 2010.

[2] http://http://wires.wiley.com (12-07-2012).

[3] D. A. Tomalia and J. M. J. Fréchet. *Journal of Polymer Science: Part A: Polymer Chemistry*, 40:2719–2728, 2002.

[4] H. Ihre, A. Hult, J. M. J. Fréchet, and I. Gitsov. *Macromolecules*, 31:4061–4068, 1998.

[5] K. T. Oh, H. Yin, E. S. Lee, and Y. H. Bae. *J. Mater. Chem.*, 17:3987–4001, 2007.

[6] L. Tian and P. T. Hammond. *Chemistry of Materials*, 18:3976–3984, 2006.

[7] American Cancer Society. *Cancer Facts and Figures*, 2012.

[8] W. M Saltzman. *Biomedical Engineering*. Cambridge University Press, 2009.

[9] P. Bawa, V. Pillay, Y. E. Choonara, and L. C. du Toit. *Biomedical Materials*, 4:1–15, 2009.

[10] B. D. Ratner, A. S. Hoffman, F. J. Schoen, and J. E. Lemons. *Biomaterials Science: An introduction to materials in medicine*. Academic Press, 1996.

[11] M. Calderon, M. A. Quadir, M. Strumia, and R. Haag. *Biochimie*, 92:1242–1251, 2010.

[12] R. A. Petros and J. M. DeSimone. *Nature Reviews*, 9:615–627, 2010.

[13] S.R. MacEwan, D. J. Callahan, and A. Chilkoti. *Nanomedicine*, 5:793–806, 2010.

[14] L. Ilium, S. S. Davis, C. G. Wilson, N. W. Thomas, M. Frier, and J. G. Hard. *International Journal of Pharmaceutics*, 12:135–146, 1982.

[15] J. H. Park, S. Lee, J. H. Kim, K. Park, K. Kim, and I. C. Kwon. *Prog. Polym. Sci.*, 33:113–137, 2008.

[16] Y. Li, Y.; Pei, X. Zhang, X. Gu, Z. Zhou, W. Yuan, J. Zhou, J. Zhu, and X. Gao. *Journal of Controlled Release*, 16:195–214, 1995.

[17] E. Forssen and M. Willis. *Advanced Drug Delivery Reviews*, 29:249–271, 1998.

[18] E. Buhleier, W. Wehner, and F. Vögtle. *Synthesis*, 55:155–158, 1978.

[19] D. A. Tomalia, H. Baker, J. Dewald, M. Hall, G. Kallos, S. Martin, J. Roeck, J. Ryder, and P. Smith. *Polymer Journal*, 17:117–132, 1985.

[20] G. R. Newkome, C. N. Moorefield, and F Vögtle. *Dendrimers and dendrons*. Wiley-VCH Verlag GmbH, 2001.

[21] K. Inoue. *Prog. Polym. Sci.*, 25:453–571, 2000.

[22] T. H. Mourey, S. R. Turner, M. Rubinstein, J. M. J. Fréchet, C. J. Hawker, and K. L. Wooley. *Macromolecules*, 25:2401–2406, 1992.

[23] C. J. Hawker and F. Chu. *Macromolecules*, 29:4370–4380, 1996.

[24] D. A. Tomalia. *Aldrichimica Acta*, 37:39–57, 2004.

[25] J. F. G. A. Jansen, E. M. M. de Brabander van den Berg, and E. W. Meijer. *Science*, 266:1226–1229, 1994.

[26] S. Nummelin, M. Skrifvars, and K. Rissanen. *Top. Curr. Chem.*, 210:1–58, 2000.

[27] F. Wurm and H. Frey. *Prog. Polym. Sci.*, 36:1–52, 2011.

[28] A. Carlmark, C. Hawker, A. Hult, and M. Malkoch. *Chemical Society Reviews*, 38:352–362, 2009.

[29] H. Ihre, O. L. P. De Jesus, and J. M. J. Fréchet. *J. Am. Chem. Soc.*, 123:5908–5917, 2001.

[30] G. R. Newkome, Z. Yao, G. R. Baker, and V. K Gupta. *Journal of Organic Chemistry*, 50:2003–2004, 1985.

[31] C. Hawker and J. M. J. Fréchet. *J. Chem. Soc., Chem. Commun.*, 15:110–113, 1990.

[32] H. Ihre, A. Hult, and E. Söderlind. *J. Am. Chem. Soc.*, 118:6388–6395, 1996.

[33] R. Duncan and L. Izzo. *Advanced Drug Delivery Reviews*, 57:2215–2237, 2005.

[34] N. Malik, R. Wiwattanapatapee, R. Klopsch, K. Lorenz, H. Frey, J. W. Weener, E. W. Meijer, W. Paulus, and R. Duncan. *Journal of Controlled Release*, 65:133–148, 2000.

[35] O. L. Padilla De Jesús, H. R. Ihre, L. Gagne, J. M. J. Fréchet, and F. C. Szoka. *Bioconjugate Chem.*, 13:453–461, 2002.

[36] D. Schmaljohann. *Advanced Drug Delivery Reviews*, 58:1655–1670, 2006.

[37] H. I. Lee, J. A. Lee, Z. Poon, and P. T. Hammond. *Chem. Commun.*, 32:3726–3728, 2008.

[38] H. Vihola, A. Laukkanen, H. Tenhu, and J. Hirvonen. *Journal of Pharmaceutical Sciences*, 97:4783–4793, 2008.

[39] A. M. Ponce, Z. Vujaskovic, F. Yuan, D. Heedham, and M. W. Dewhirst. *Int. J. Hyperthermia*, 22:205–213, 2006.

[40] E. E. Makhaeva, H. Tenhu, and A. R. Khokhlov. *Macromolecules*, 31:6112–6118, 1998.

[41] I. R. Nasimova, E. E. Makhaeva, and A. R. Khokhlov. *Journal of Applied Polymer Science*, 81:3238–3243, 2001.

[42] I. Galaev and B. Mattiasson, editors. *Smart Polymers: applications in biotechnology and biomedicine*. CRC Press, 2nd edition, 2008.

[43] J. F. Mano. *Advanced Engineering Materials*, 10:515–527, 2008.

[44] H. Vihola, A. Laukkanen, L. Valtola, H. Tenhu, and J. Hirvonen. *Biomaterials*, 26:3055–3064, 2005.

[45] J. Hu and S. Liu. *Macromolecules*, 43:8315–8330, 2010.

[46] I. Gitsov and J. M. J. Fréchet. *Macromolecules*, 26:6536–6546, 1993.

[47] H. A. Klok, J. J. Hwang, J. D. Hartgerink, and S. I. Stupp. *Macromolecules*, 35:6101–6111, 2002.

[48] B. Guo, X. Y. Sun, Y. F. Zhou, and D. Y. Yan. *Sci. China Chem.*, 53:487–294, 2010.

[49] J. Qiu, B. Carleux, and K. Matyjaszewski. *Prog. Polym. Sci.*, 26:2083–2134, 2001.

[50] C. Boyer, V. Bulmus, T. P. Davis, V. Ladmiral, J. Q. Liu, and S. Perrier. *Chemical Reviews*, 109:5402–5436, 2009.

[51] W. A. Braunecker and K. Matyjaszewski. *Prog. Polym. Sci.*, 32:93–146, 2007.

[52] H. C. Kolb, M. G. Finn, and K. B. Sharpless. *Angew. Chem. Int. Ed.*, 40:2004–2021, 2001.

[53] V. V. Rostovtsev, L. G. Green, V. V. Fokin, and K. B. Sharpless. *Angew. Chem. Int. Ed.*, 41:2596–2599, 2002.

[54] J. F. Lutz. *Angew. Chem. Int. Ed.*, 46:1018–1025, 2007.

[55] A. Sharma, K. Neibert, R. Sharma, R. Hourani, D. Maysinger, and A. Kakkar. *Macromolecules*, 44:521–529, 2011.

[56] L. Liang and D. Astruc. *Coordination Chemistry Reviews*, 255:2933–2945, 2011.

[57] H. Burrows and M. Pereira. *Química - Síntese e Estrutura Uma Abordagem Prática*. Escolar Editora, 2006.

[58] R. Morrison and R. Boyd. *Química Orgânica*. Fundação Calouste Gulbenkian, 2005.

[59] J. S. Moore and S. I. Stupp. *Macromolecules*, 23:65–70, 1990.

[60] P. Wu, M. Malkoch, J. N. Hunt, R. Vestberg, E. Kaltgrad, M. G. Finn, V. V. Fokin, K. B. Sharpless, and C. J. Hawker. *Chem. Commun.*, pages 5775–5777, 2005.

[61] J. del Barrio, L. Oriol, R. Alcalá, and C. Sánchez. *Macromolecules*, 42:5752–5760, 2009.

Appendix A

NMR spectra

A.1 Double-stage convergent growth approach

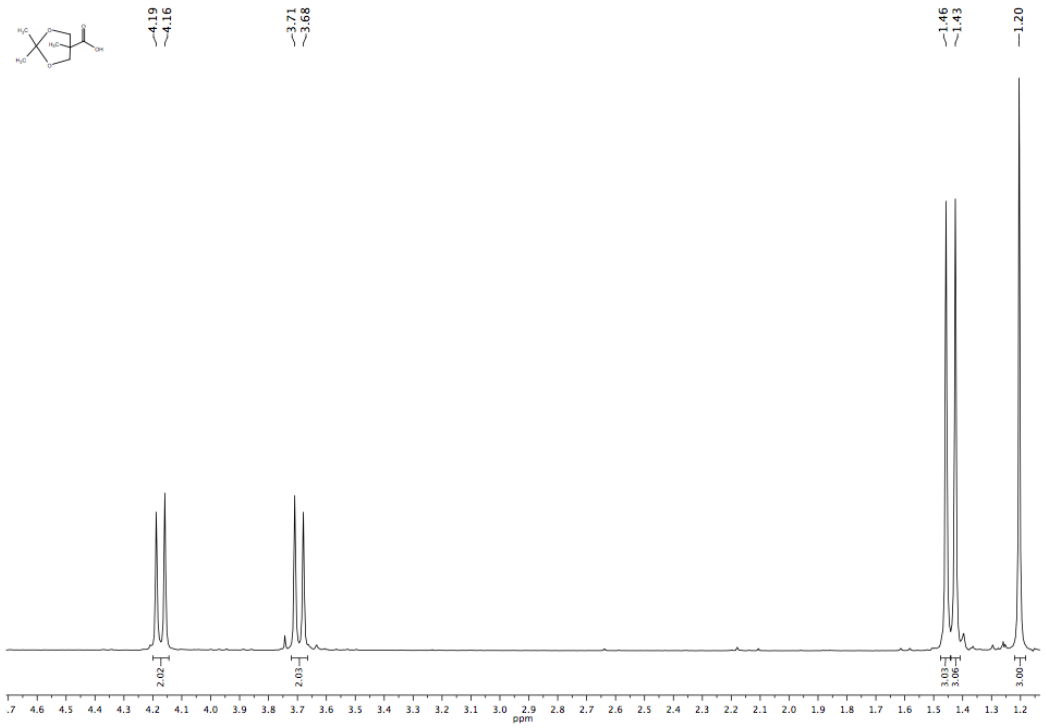

Figure A.1: ^{1}H NMR spectrum of [1].

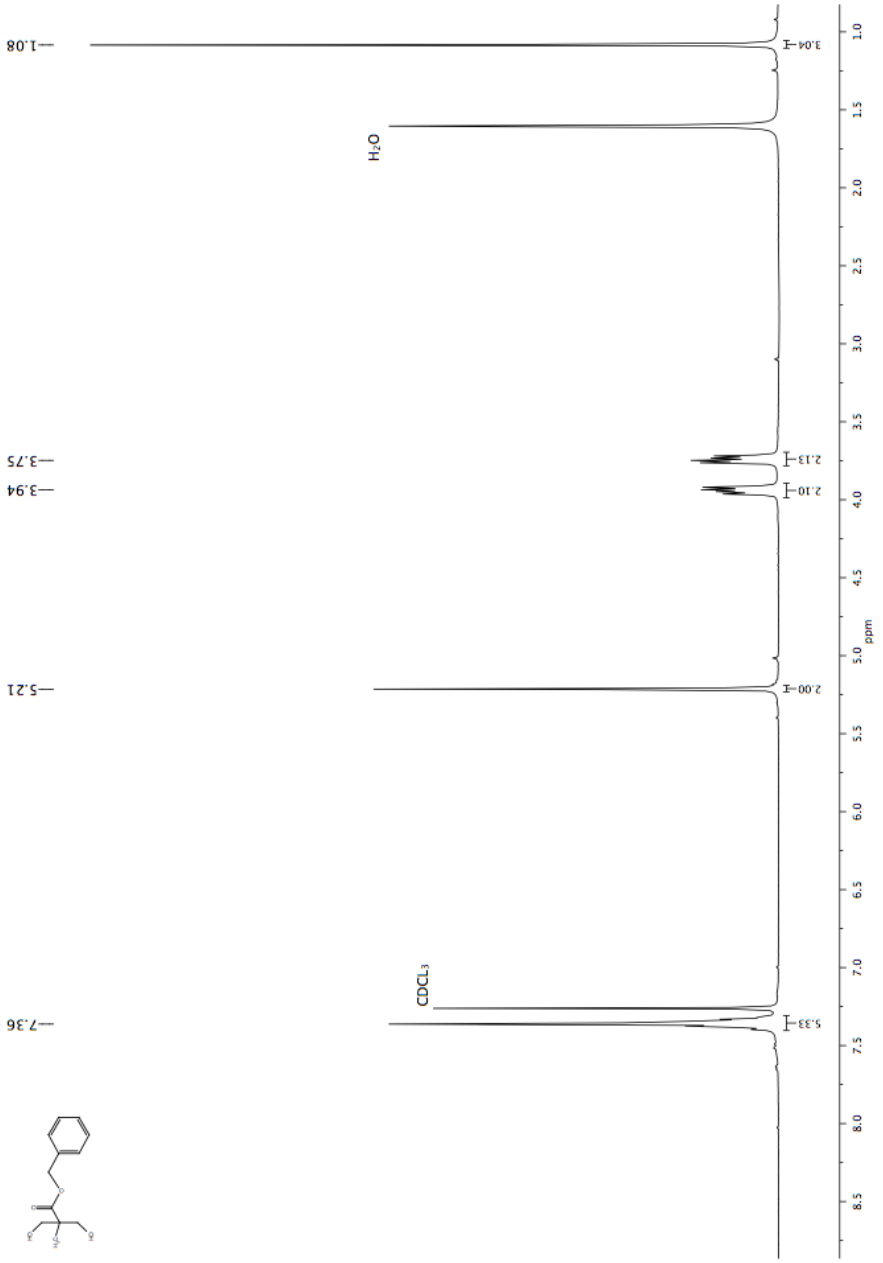

Figure A.2: ^{1}H NMR spectrum of [2].

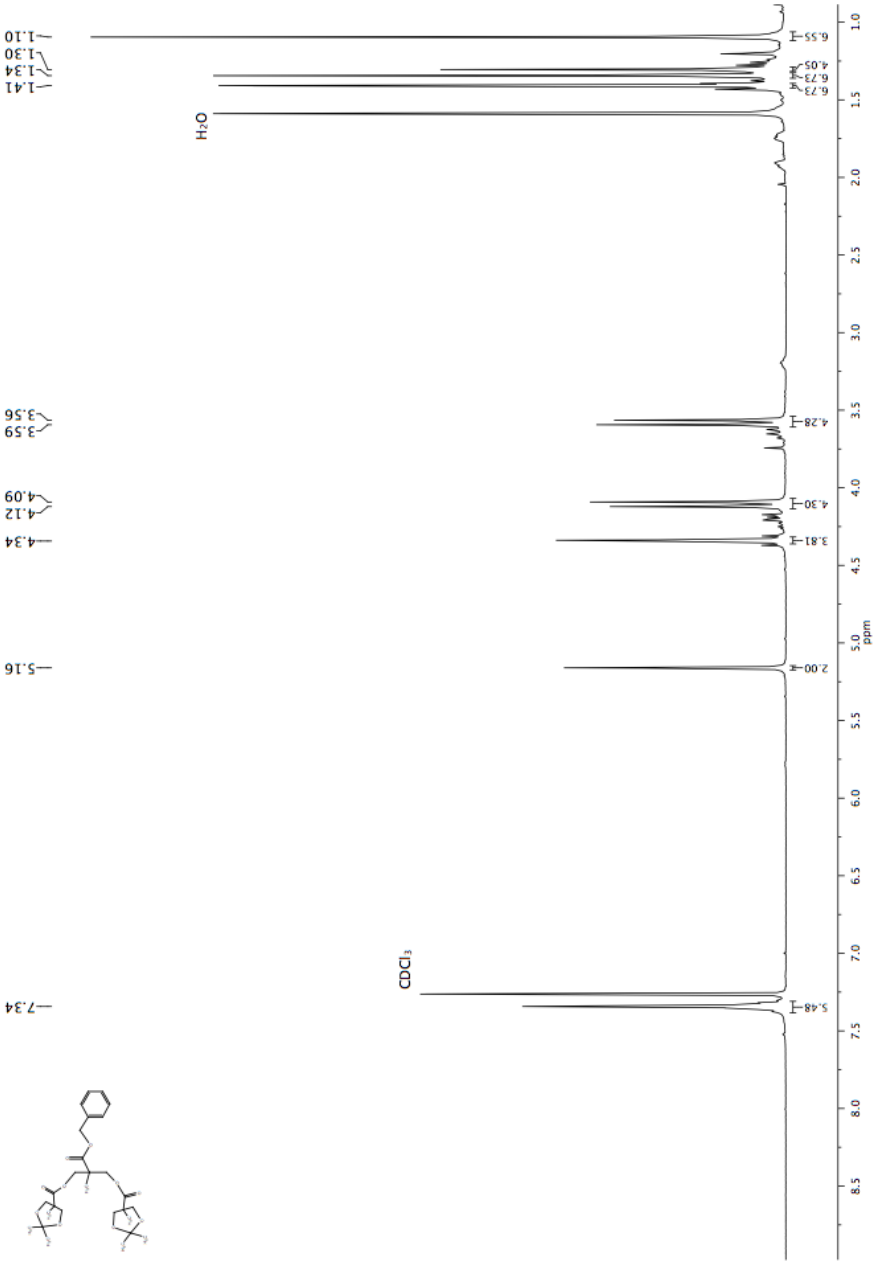

Figure A.3: ^{1}H NMR spectrum of [3].

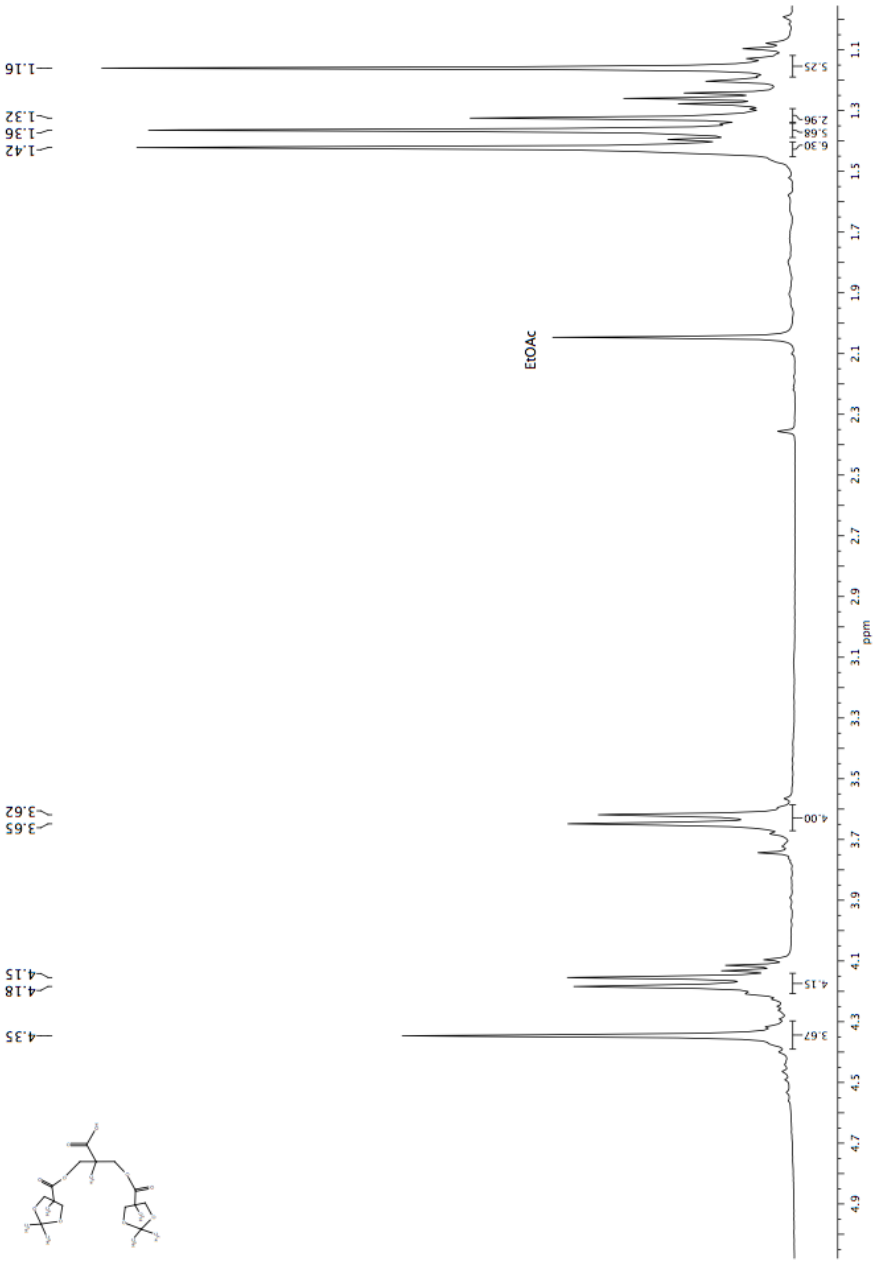

Figure A.4: ^{1}H NMR spectrum of [4].

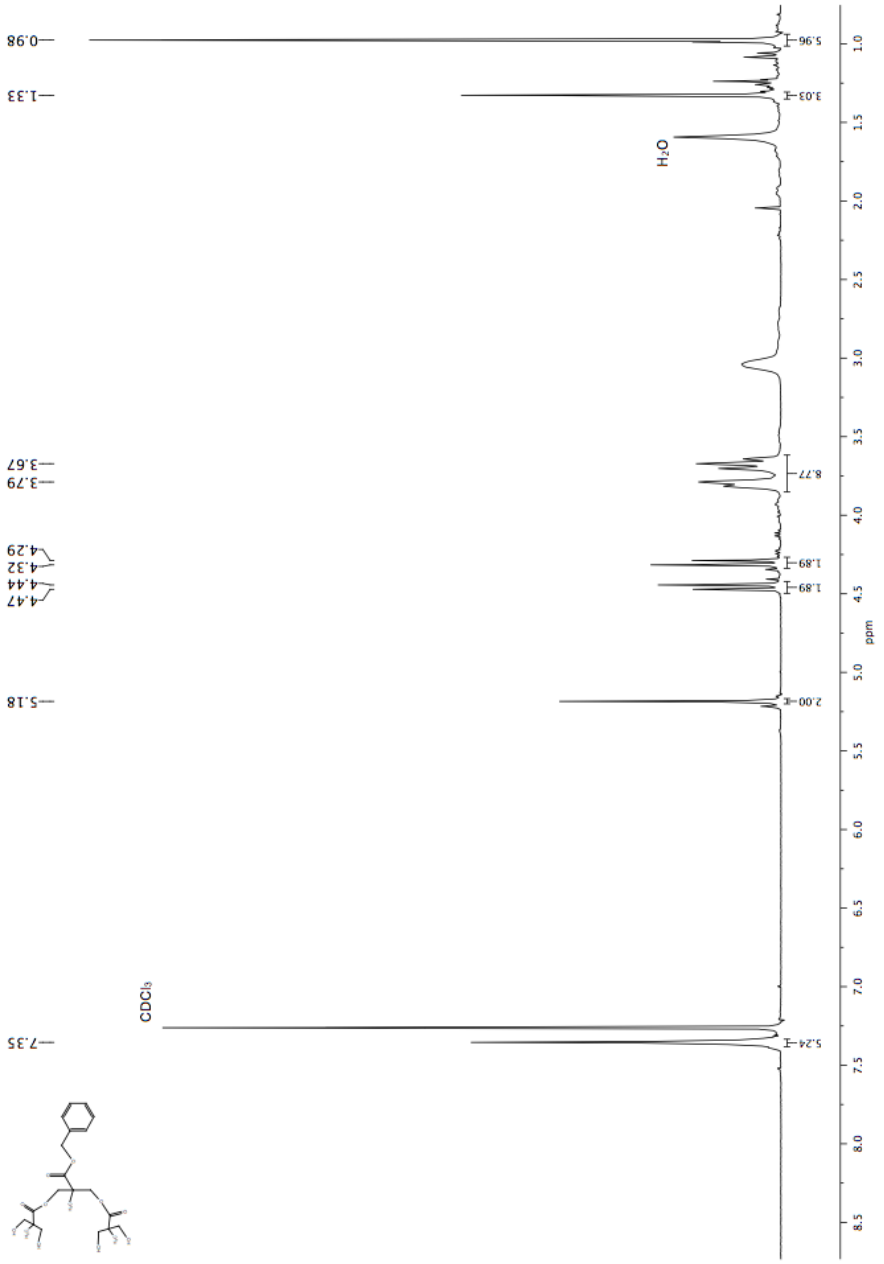

Figure A.5: ^{1}H NMR spectrum of [5].

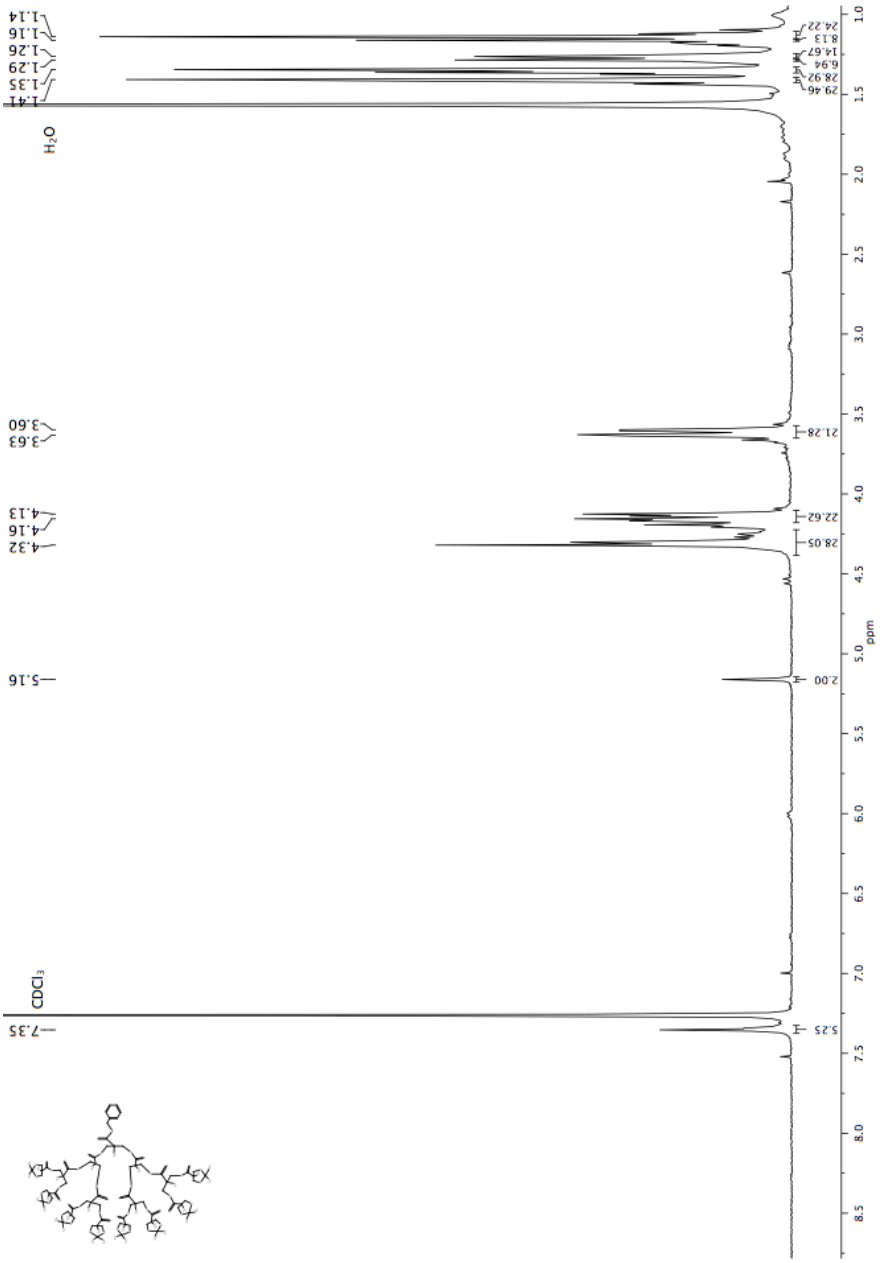

Figure A.6: ^{1}H NMR spectrum of [6].

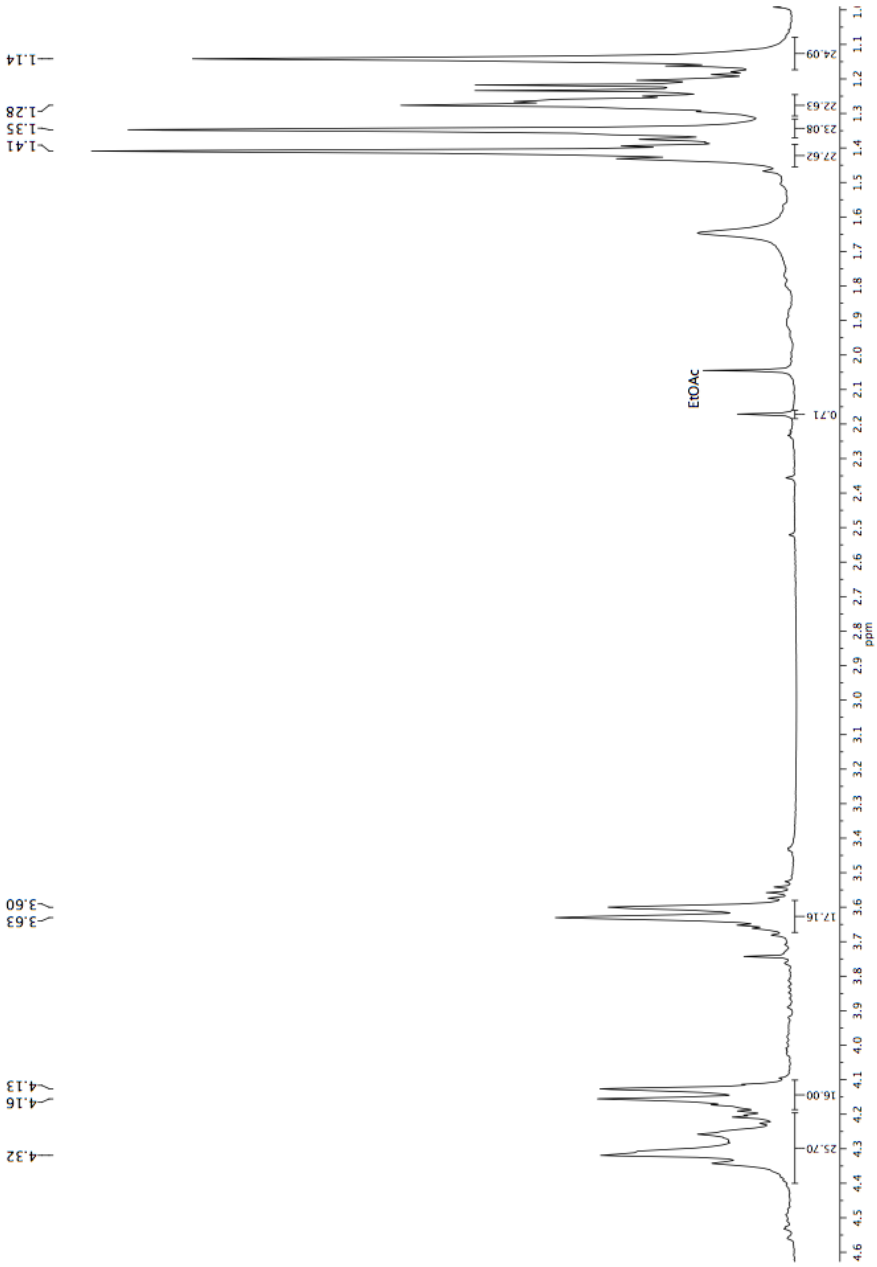

Figure A.7: ^{1}H NMR spectrum of entry #1.

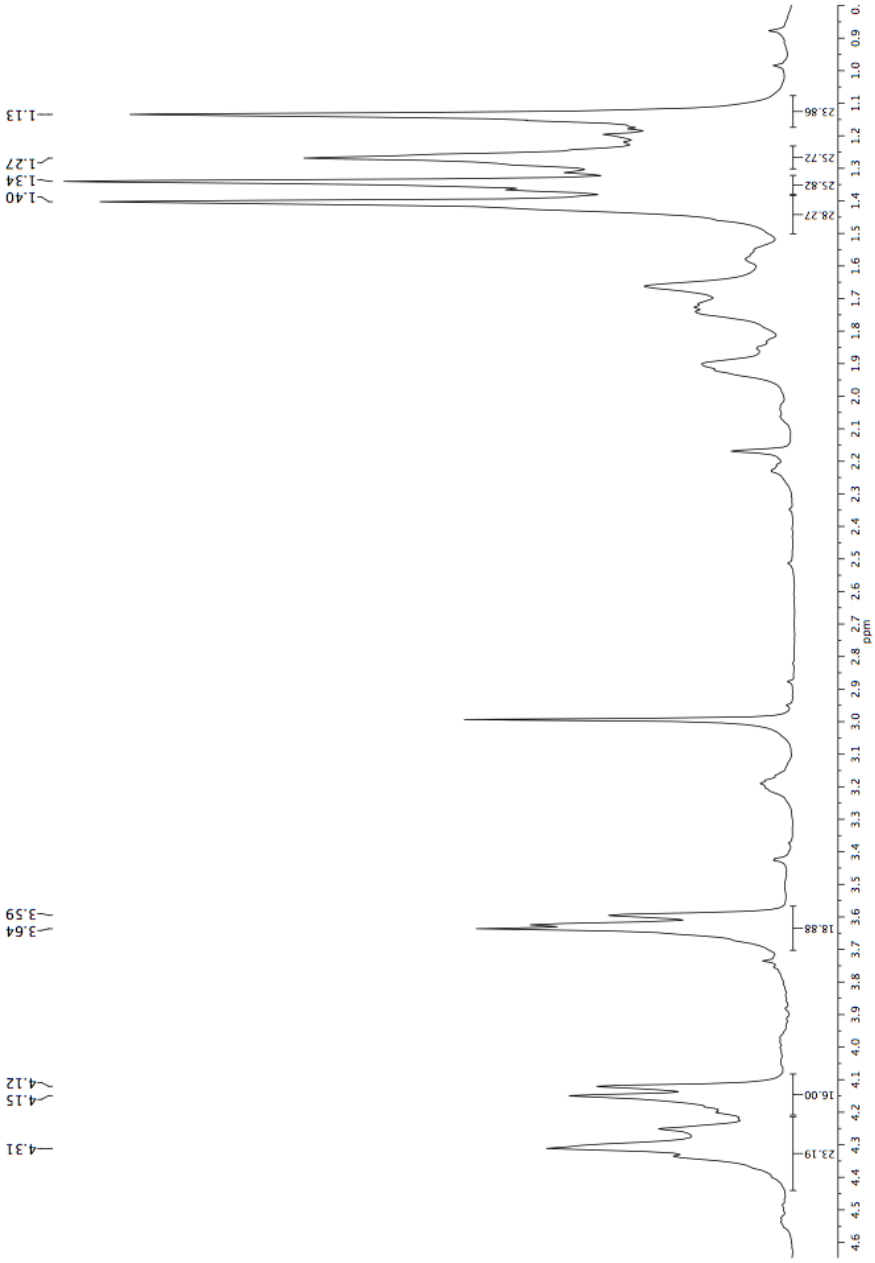

Figure A.8: ^{1}H NMR spectrum of entry #2.

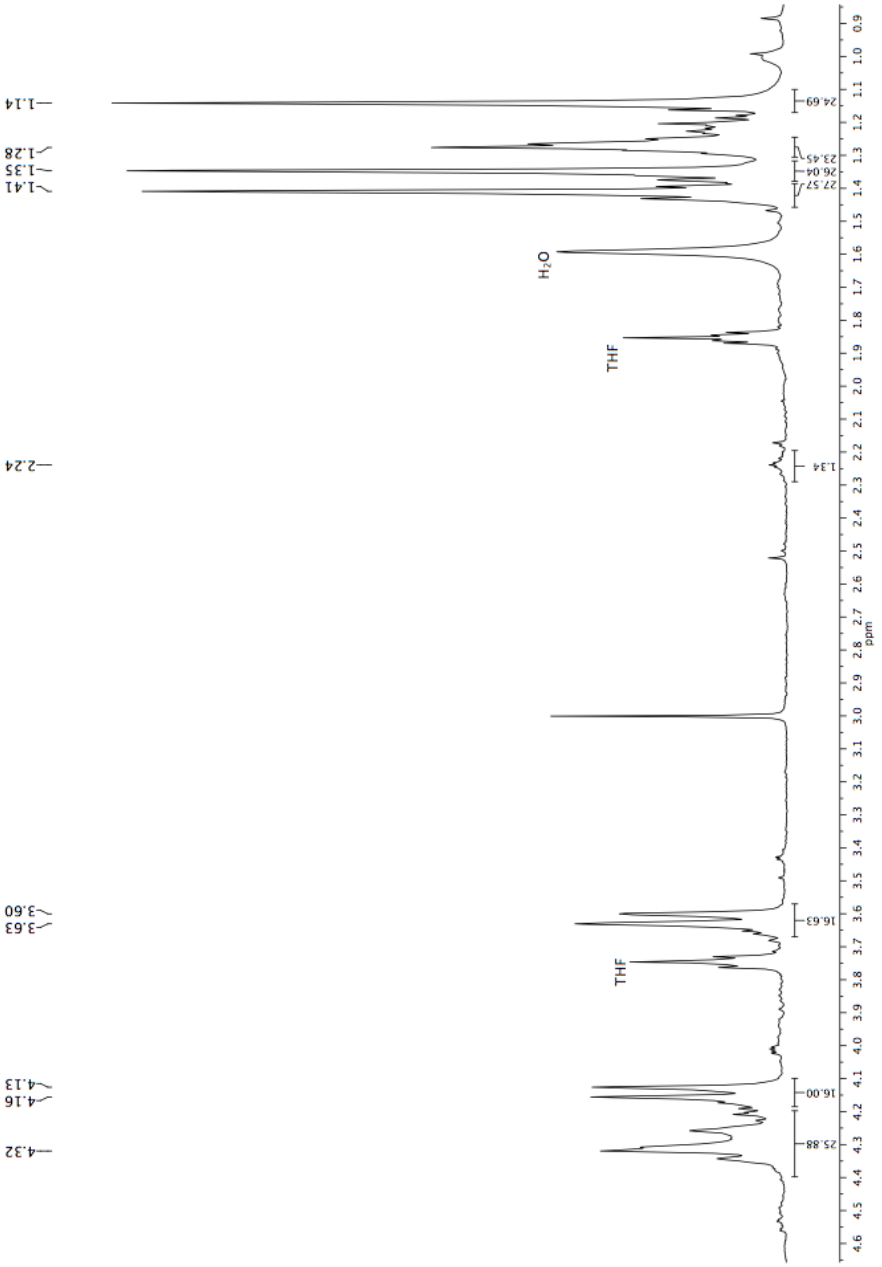

Figure A.9: ^{1}H NMR spectrum of entry #3.

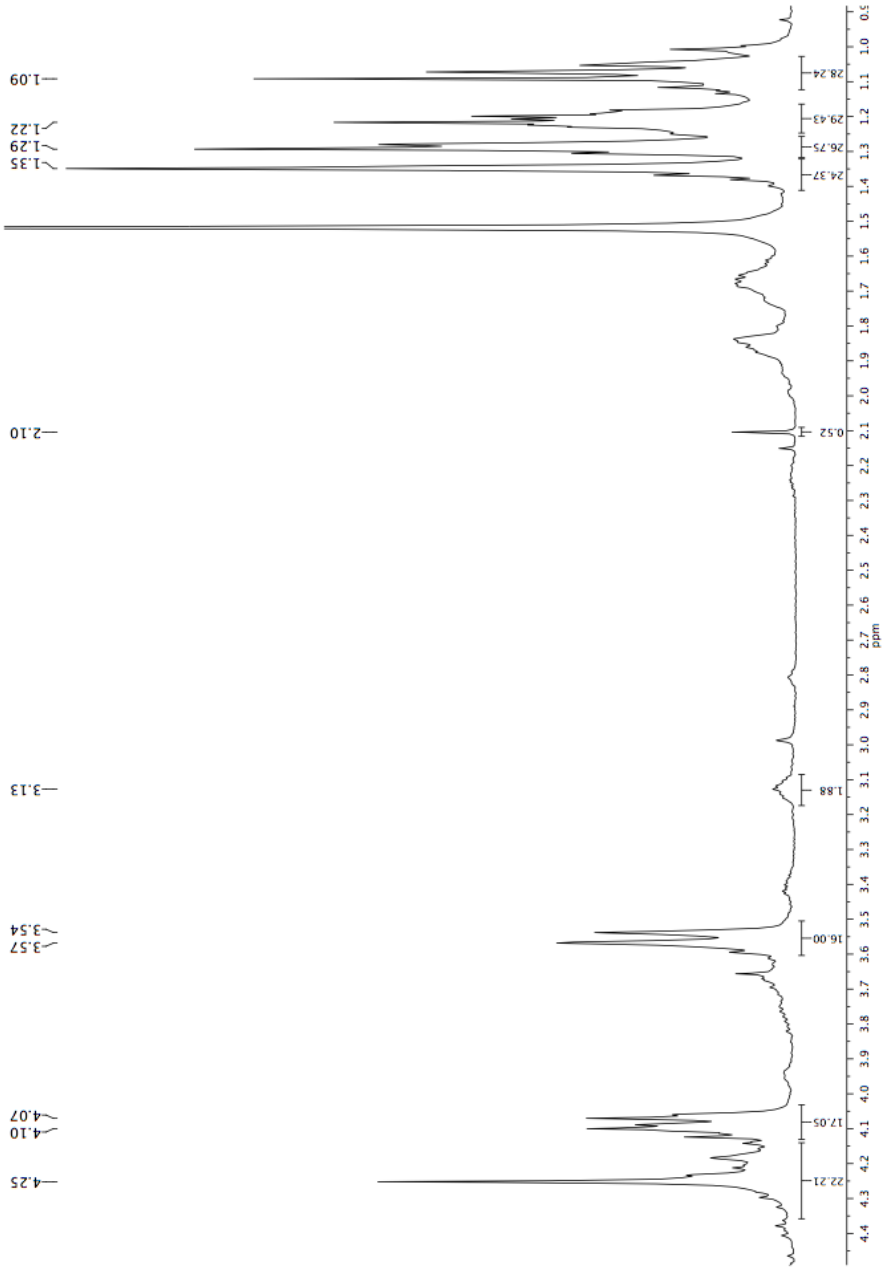

Figure A.10: ^{1}H NMR spectrum of entry #4.

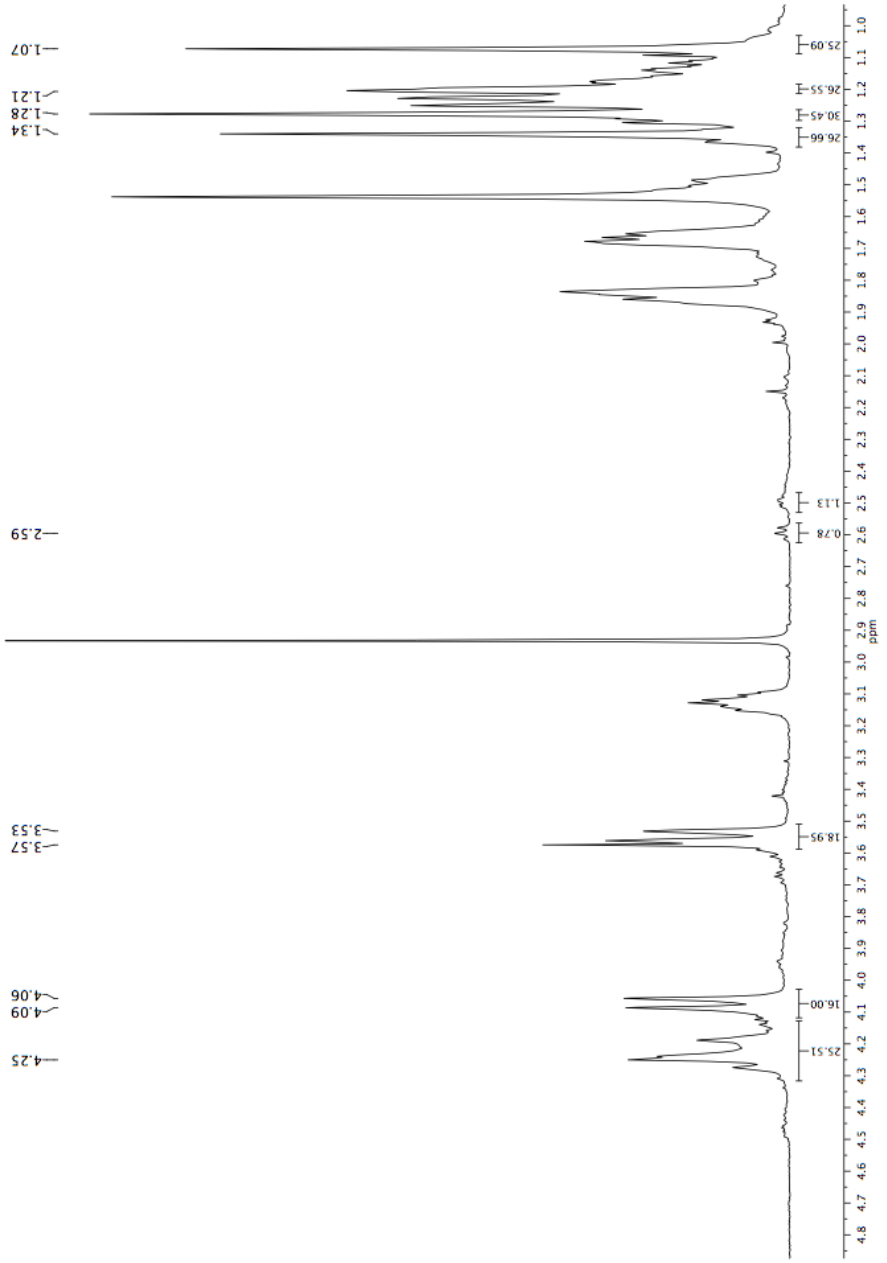

Figure A.11: ^{1}H NMR spectrum of entry #5.

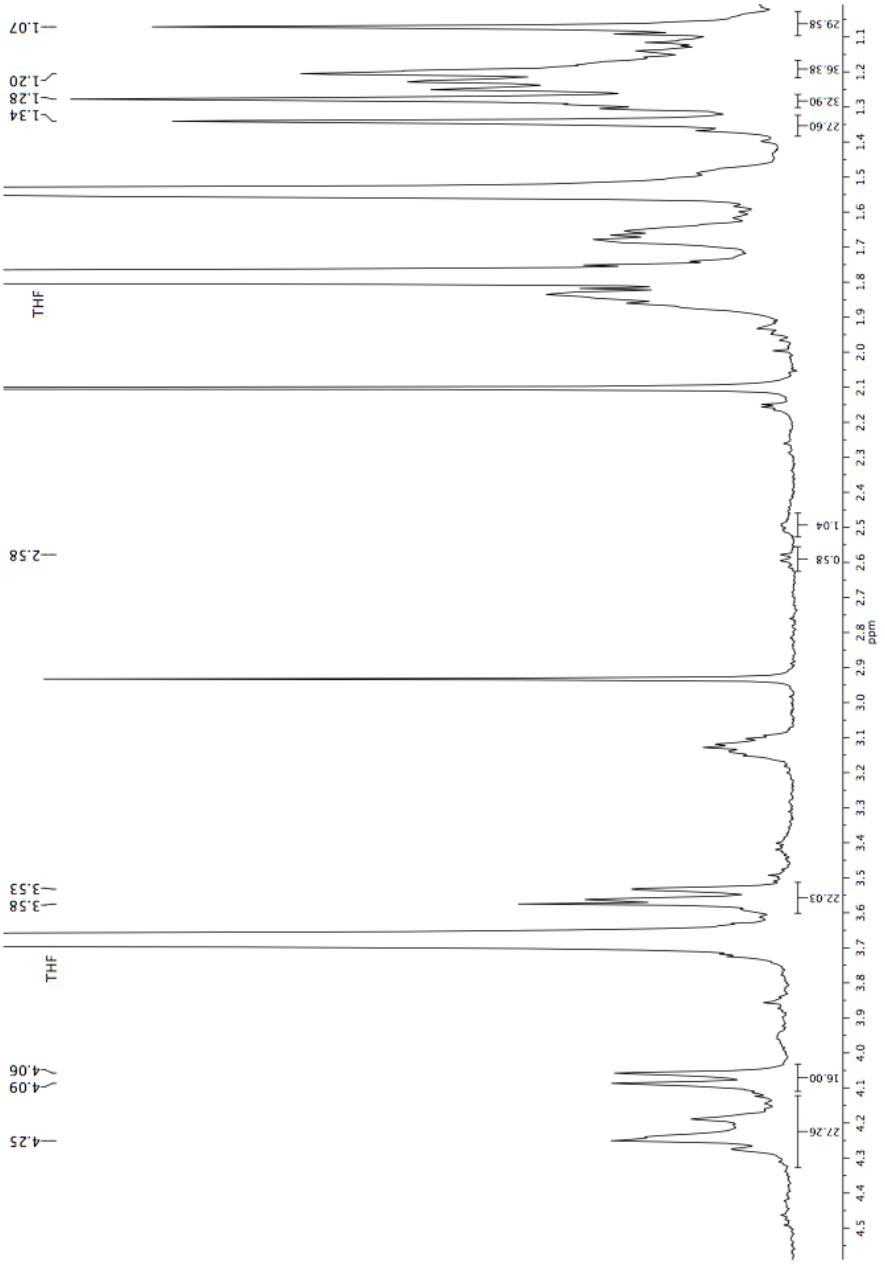

Figure A.12: ^{1}H NMR spectrum of entry #6.

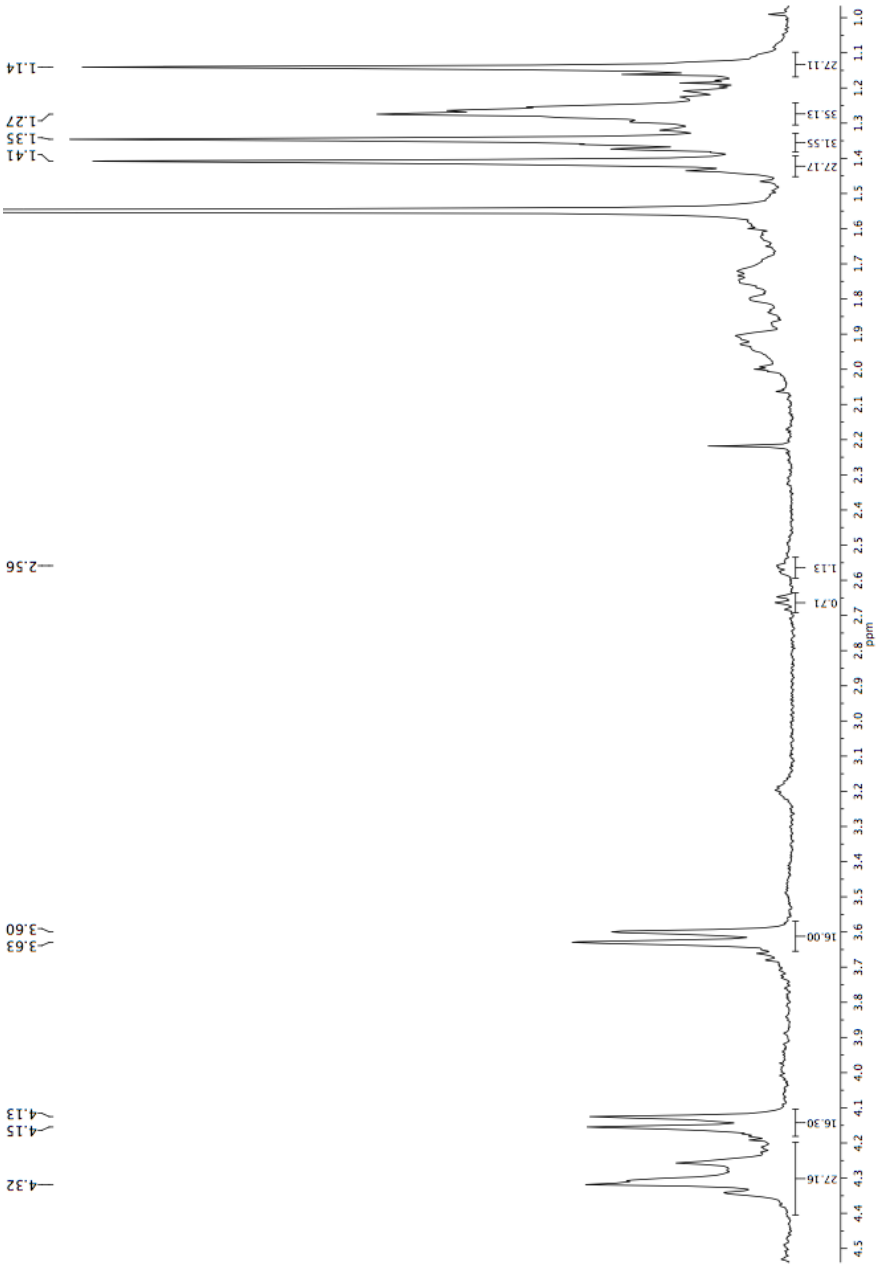

Figure A.13: ^{1}H NMR spectrum of entry #7.

Appendix B

NMR spectra

B.1 Anhydride route

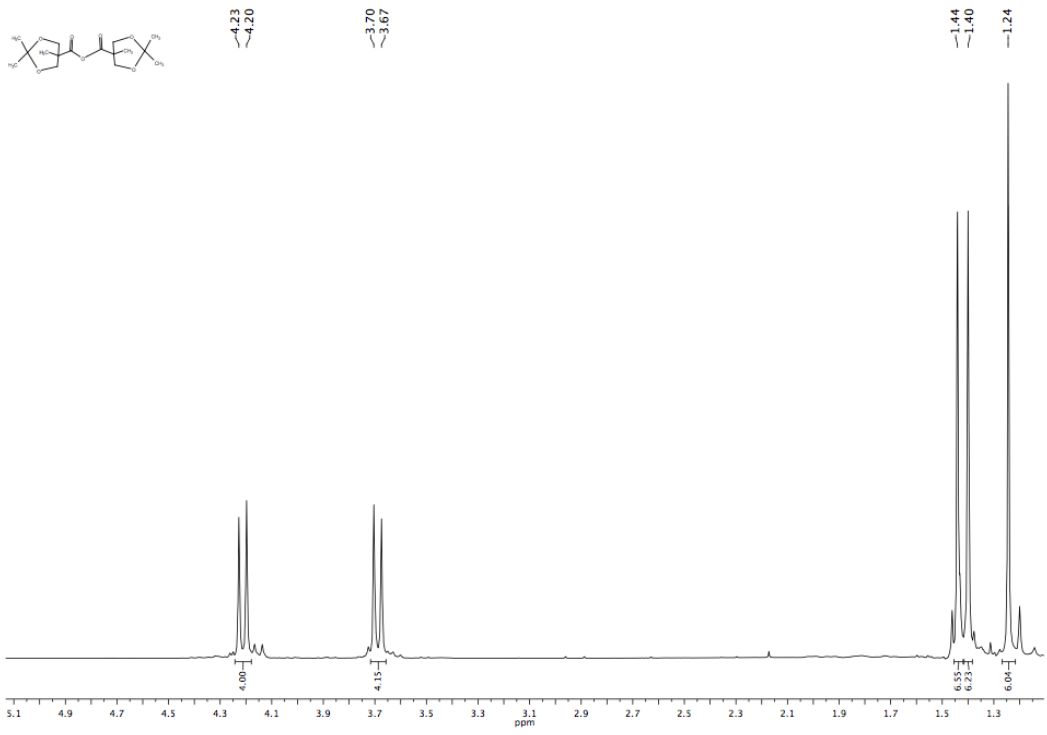

Figure B.1: ^{1}H NMR spectrum of [A1].

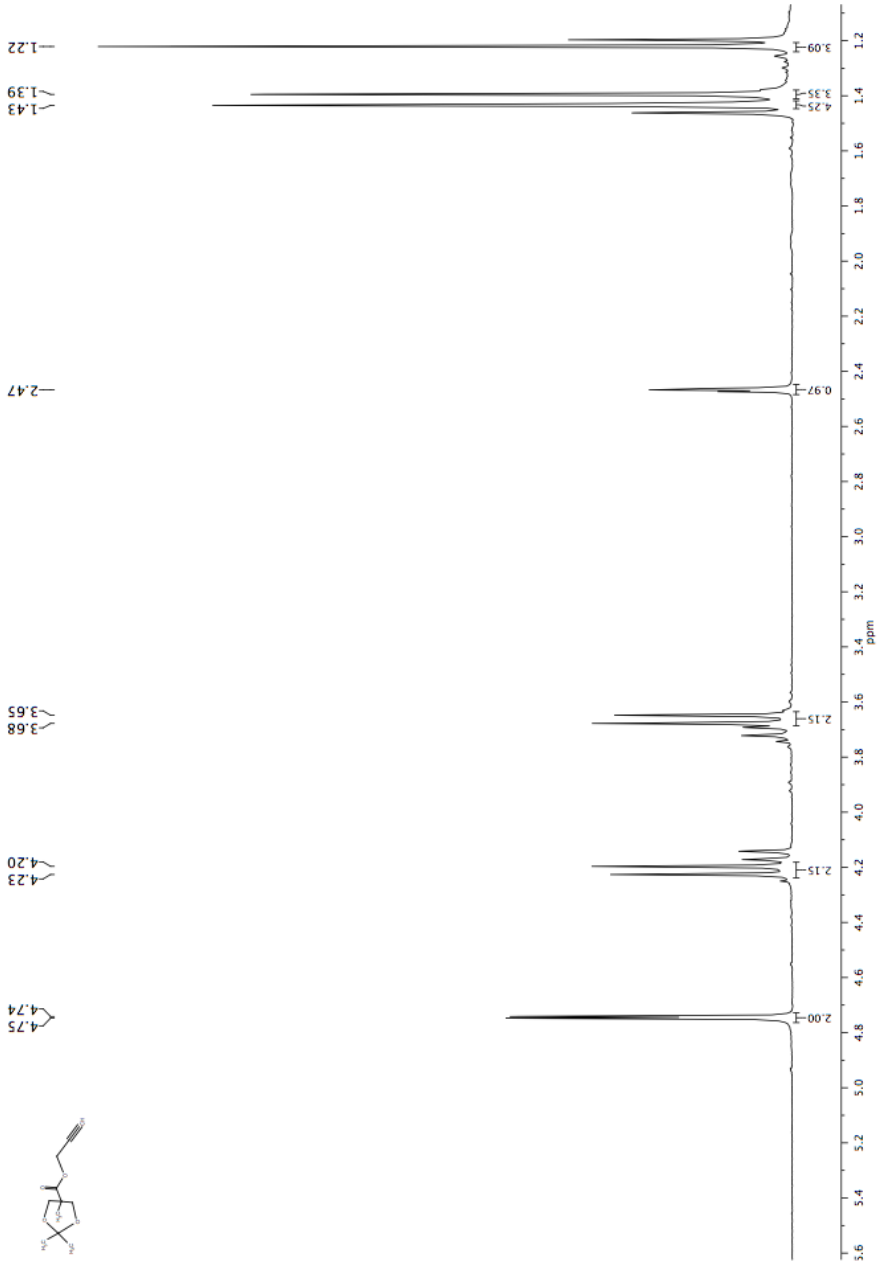

Figure B.2: ^{1}H NMR spectrum of [A2].

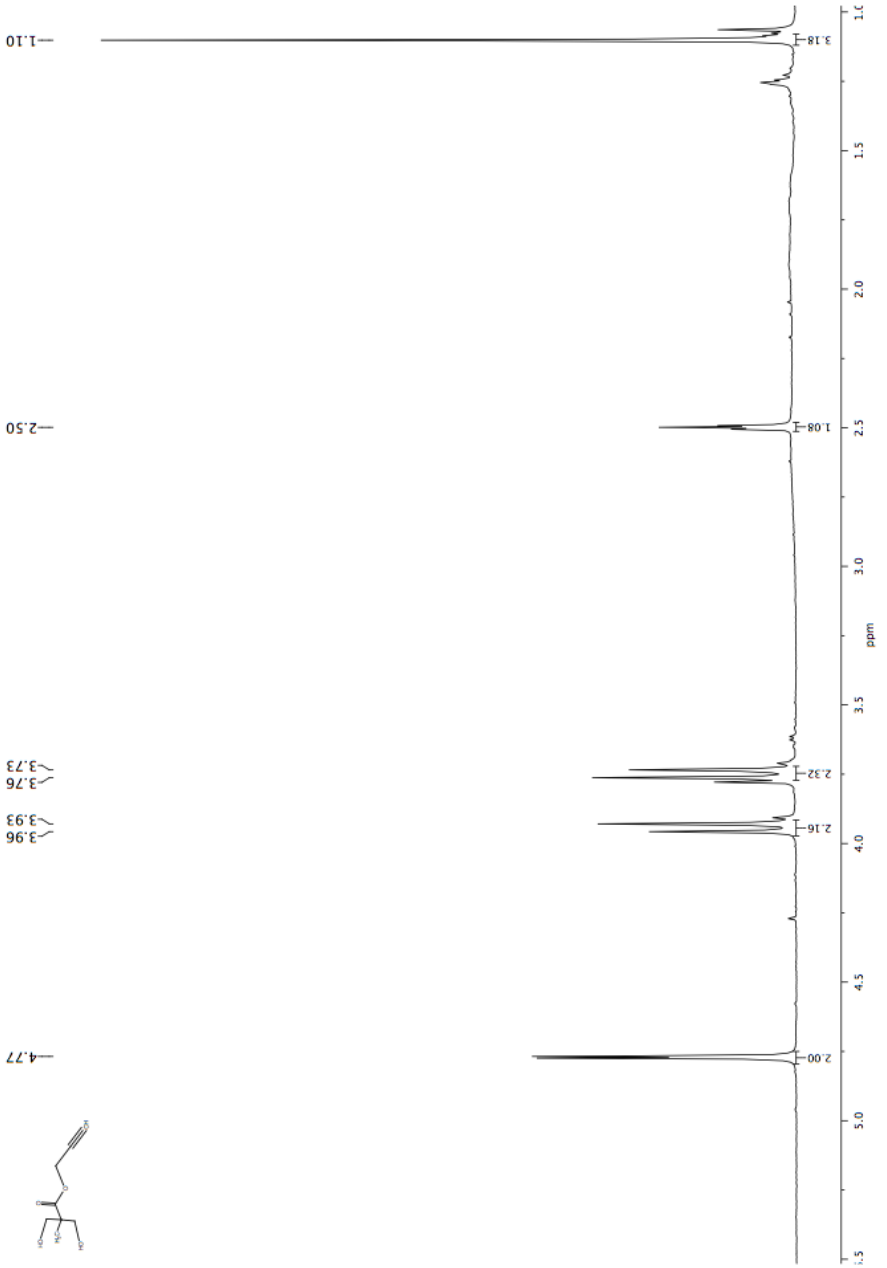

Figure B.3: ^{1}H NMR spectrum of [A3].

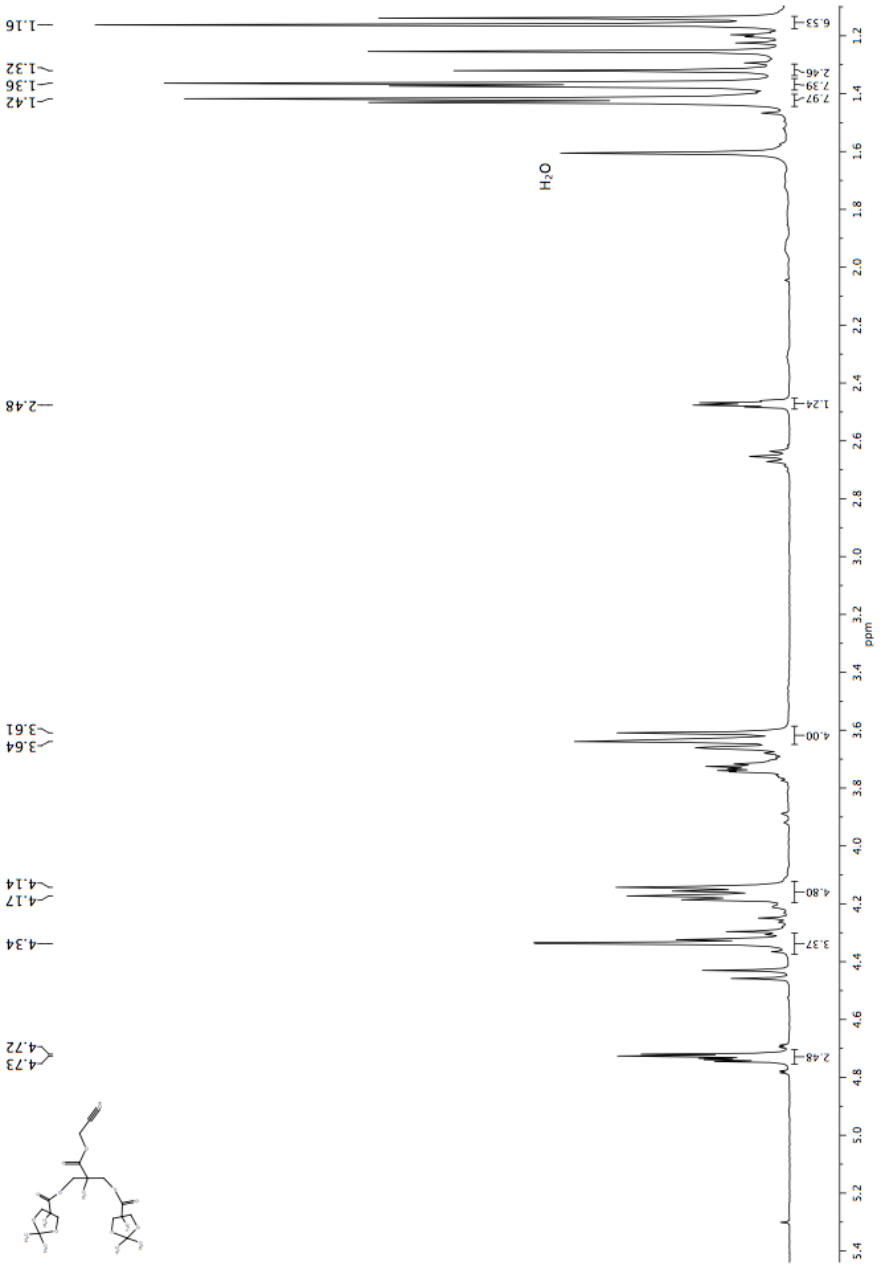

Figure B.4: ^{1}H NMR spectrum of [A4].

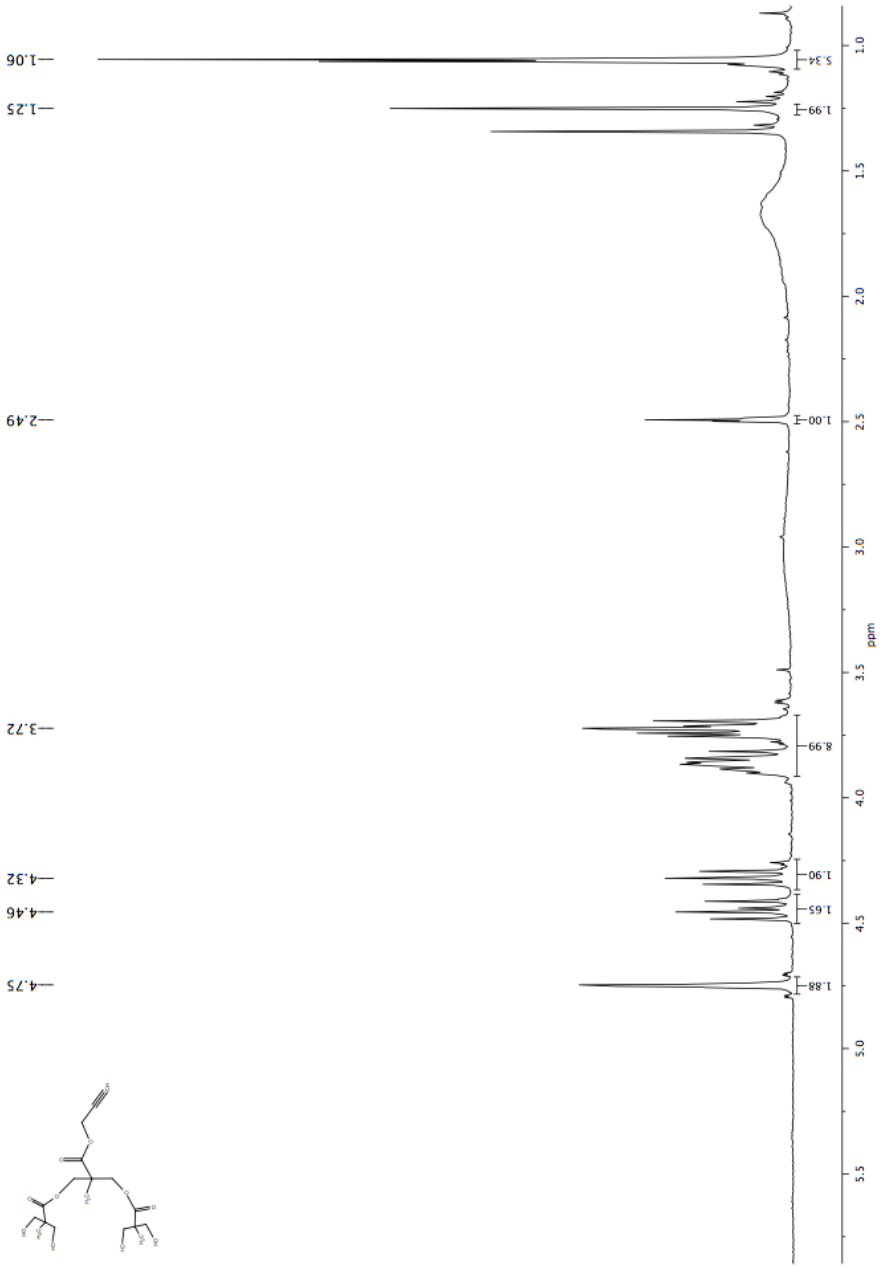

Figure B.5: ^{1}H NMR spectrum of [A5].

Appendix C

NMR and FT-IR spectra

C.1 Alkyne functionalization of PEG

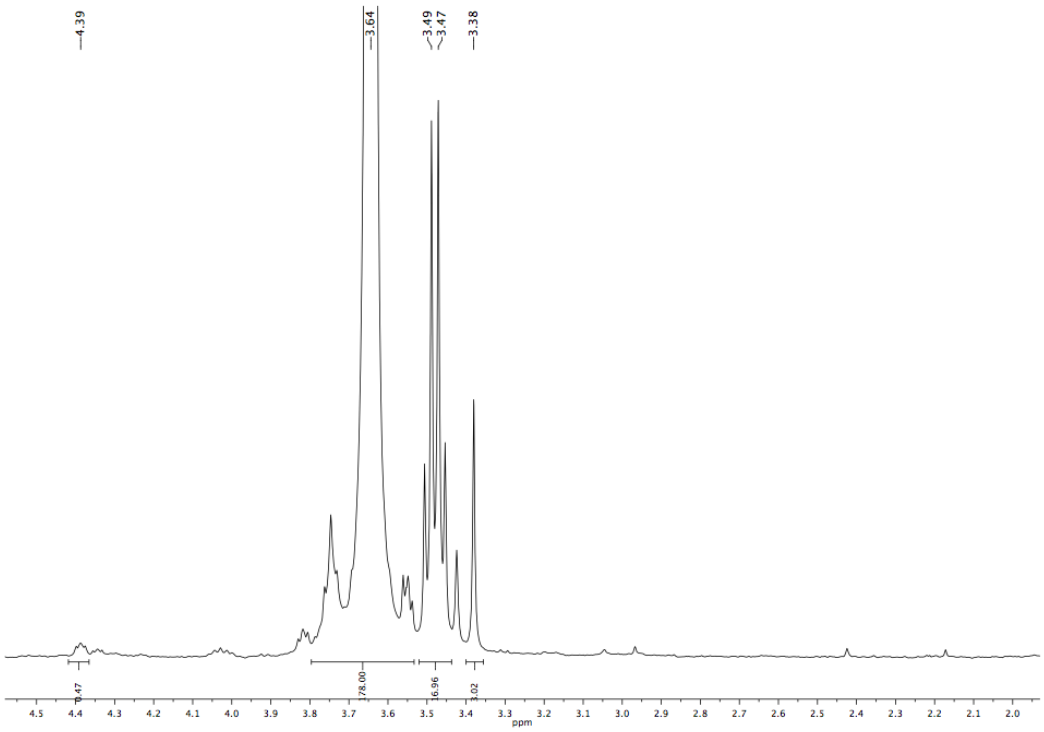

Figure C.1: ^{1}H NMR spectrum of entry #1.

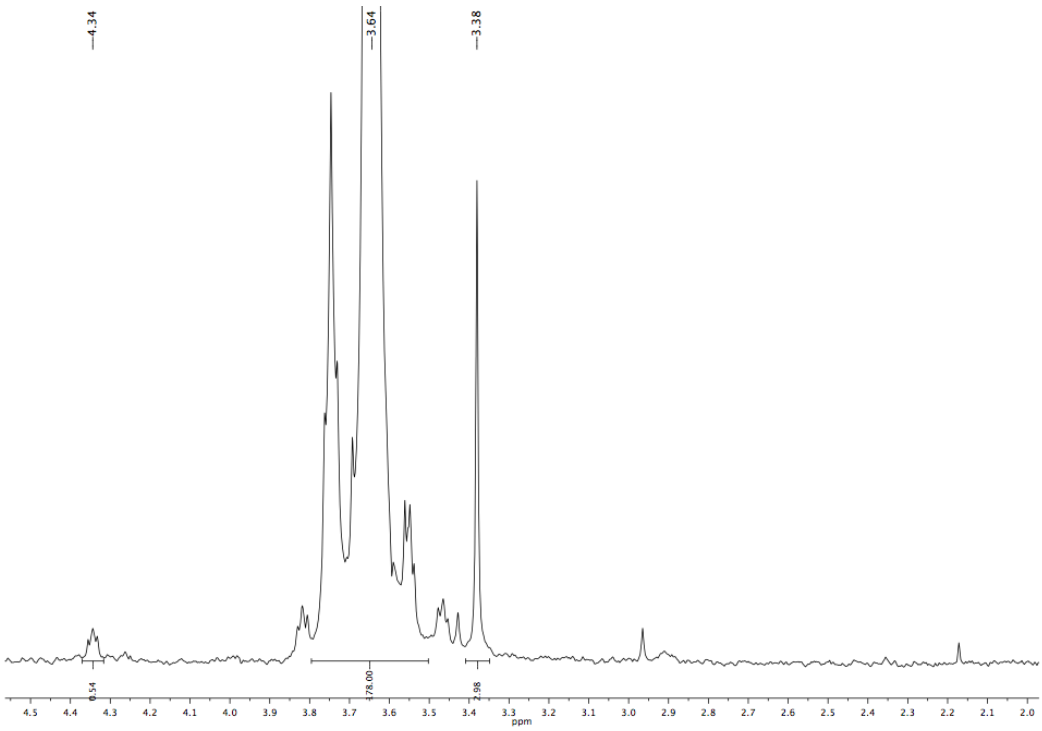

Figure C.2: ^{1}H NMR spectrum of entry #2.

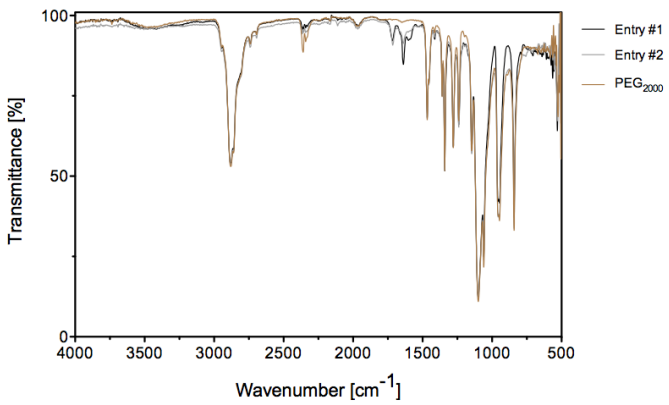

Figure C.3: ATR-FTIR transmittance spectra of #1 and #2 PEG_{2000} alkyne functionalization attempts.

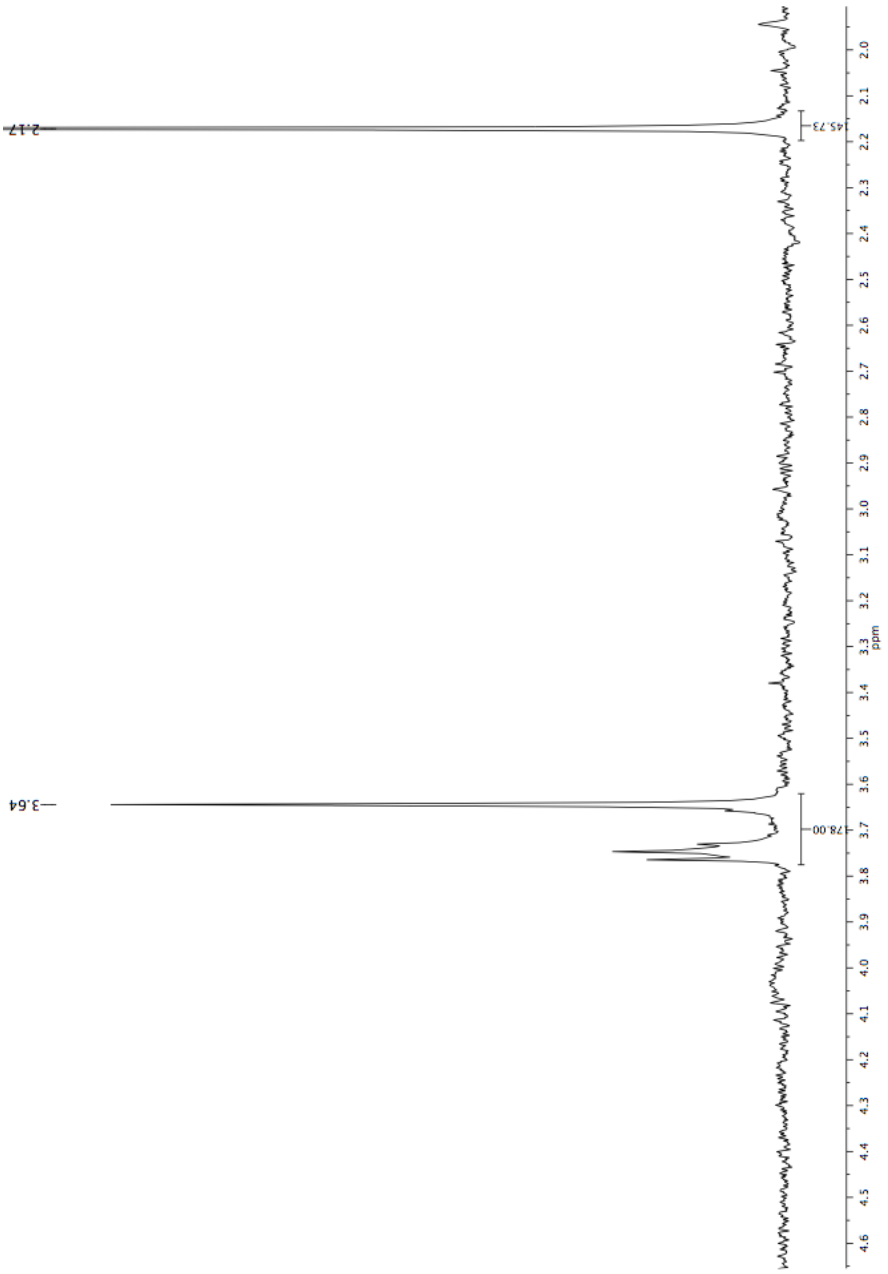

Figure C.4: ^{1}H NMR spectrum of entry #3.

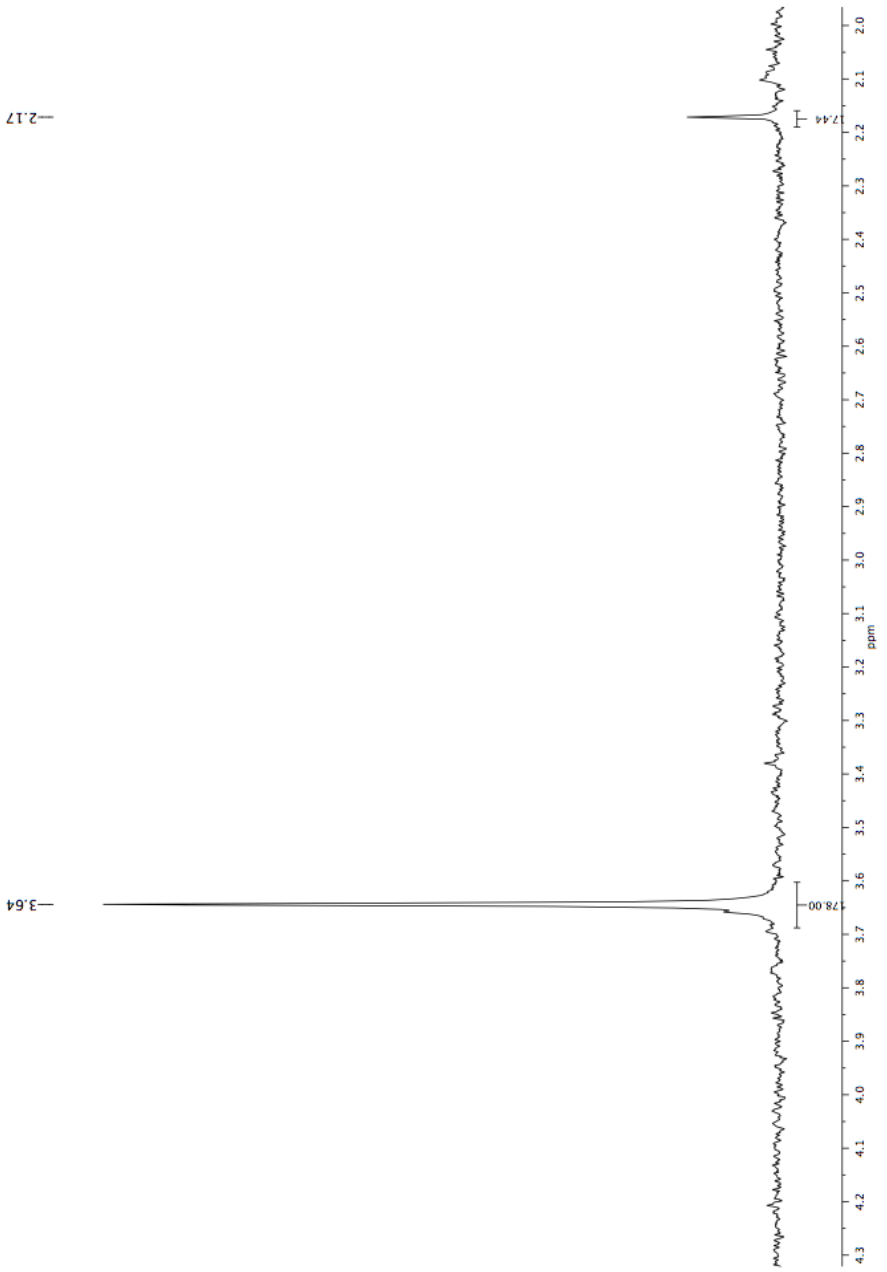

Figure C.5: ^{1}H NMR spectrum of entry #4.

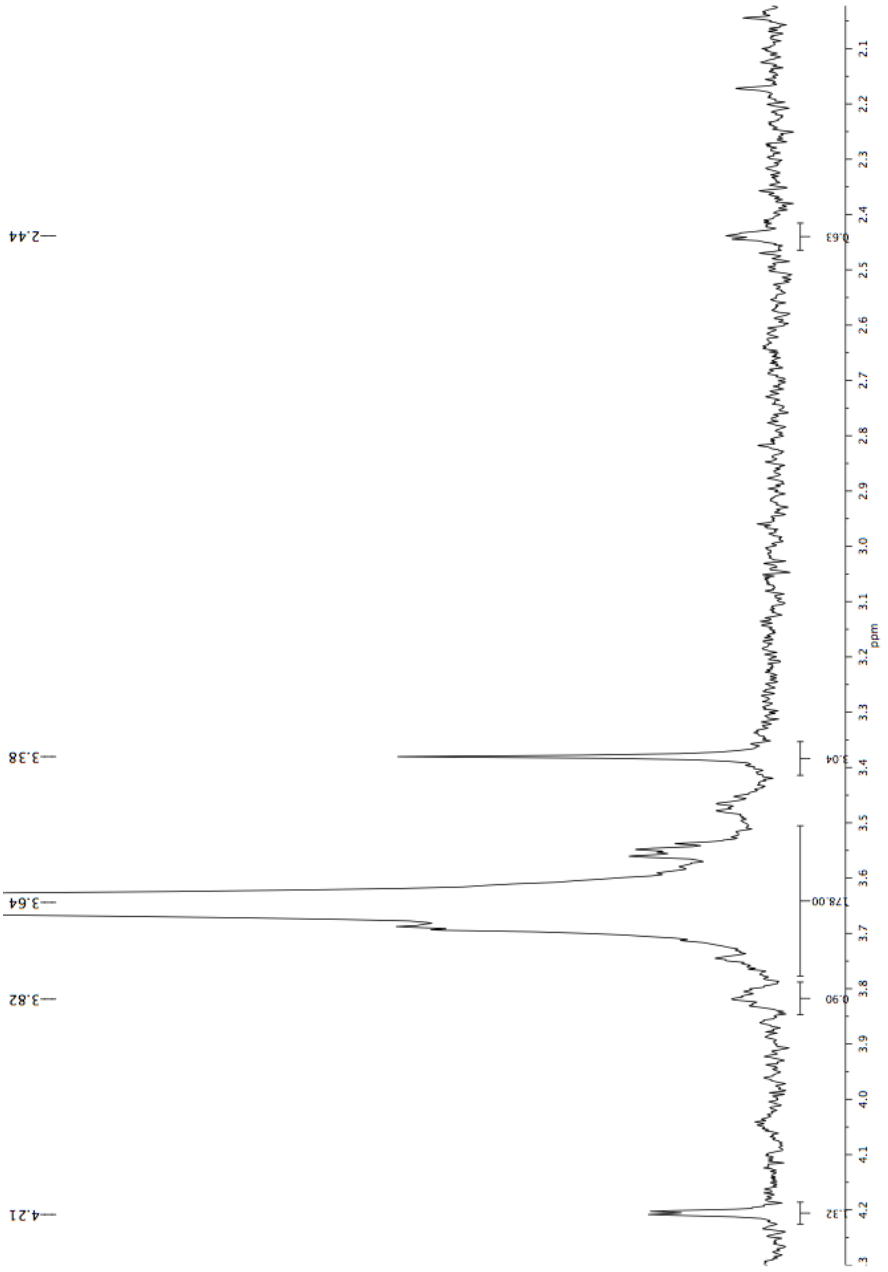

Figure C.6: ^{1}H NMR spectrum of entry #5.